Microbiome

RESEARCH

Open Access

# *Lactiplantibacillus plantarum* FRT4 protects against fatty liver hemorrhage syndrome: regulating gut microbiota and *FoxO/TLR-4/NF-κB* signaling pathway in laying hens

Daojie Li[1], Kun Meng[1], Guohua Liu[1], Zhiguo Wen[1], Yunsheng Han[1], Weiwei Liu[1], Xin Xu[1], Liye Song[1], Hongying Cai[1*] and Peilong Yang[1*]

## Abstract

**Background** Fatty liver hemorrhage syndrome (FLHS) has become one of the major factors leading to the death of laying hen in caged egg production. FLHS is commonly associated with lipid peroxidation, hepatocyte injury, decreased antioxidant capacity, and inflammation. However, there are limited evidences regarding the preventive effect of *Lactiplantibacillus plantarum* on FLHS in laying hens and its mechanisms. Our previous results showed that *Lp. plantarum* FRT4 alleviated FLHS by regulating lipid metabolism, but did not focus on its antioxidant and anti-inflammatory functions and mechanisms. Therefore, this study aimed to investigate the preventive mechanisms of *Lp. plantarum* FRT4 in alleviating FLHS, with a focus on its role in antioxidant activity and inflammation regulation.

**Results** Supplementation with *Lp. plantarum* FRT4 enhanced the levels of T-AOC, T-SOD, and GSH-Px, while reducing the levels of TNF-α, IL-1β, IL-8, and NLRP3 in the liver and ovary of laying hens. Additionally, *Lp. plantarum* FRT4 upregulated the mRNA expressions of *SOD1*, *SOD2*, *CAT*, and *GPX1*, downregulated the mRNA expressions of pro-inflammatory factors *IL-1β*, *IL-6*, and *NLRP3*, and upregulated the mRNA expressions of anti-inflammatory factors *IL-4* and *IL-10*. *Lp. plantarum* FRT4 improved the structure and metabolic functions of gut microbiota, and regulated the relative abundances of dominant phyla (Bacteroidetes, Firmicute, and Proteobacteria) and genera (*Prevotella* and *Alistipes*). Additionally, it influenced key KEGG pathways, including tryptophan metabolism, amino sugar and nucleotide sugar metabolism, insulin signaling pathway, FoxO signaling pathway. Spearman analysis revealed that the abundance of microbiota at different taxonomic levels was closely related to antioxidant enzymes and inflammatory factors. Furthermore, *Lp. plantarum* FRT4 modulated the mRNA expressions of related factors in the *FoxO/TLR-4/NF-κB* signaling pathway by regulating gut microbiota. Moreover, the levels of $E_2$, FSH, and VTG were significantly increased in the ovary after *Lp. plantarum* FRT4 intervention.

**Conclusions** *Lp. plantarum* FRT4 effectively ameliorates FLHS in laying hens. This efficacy is attributed to its antioxidant and anti-inflammatory properties, which are mediated by modulating the structure and function of gut microbiota, and further intervening in the *FoxO/TLR-4/NF-κB* signaling pathway. These actions enhance hepatic and ovarian function and increase estrogen levels.

*Correspondence:
Hongying Cai
caihongying@caas.cn
Peilong Yang
yangpeilong@caas.cn

**Keywords** Fatty liver hemorrhage syndrome, *Lactiplantibacillus plantarum* FRT4, Oxidative stress, Gut microbiota, *FoxO/TLR-4/NF-κB* signaling pathway

## Background

Fatty liver hemorrhage syndrome (FLHS) is a common disease in laying hens, also known as non-alcoholic fatty liver disease (NAFLD) or metabolic associated fatty liver disease (MAFLD) [1]. Typically, FLHS occurs during the middle and late stages of laying hens' life cycle, causing huge economic losses [2]. FLHS leads to an imbalance between the production of reactive oxygen species (ROS) and the capacity of antioxidant system [3]. The accumulation of ROS and reduction of antioxidant capacity result in oxidative stress (OS) and tissue damage [4, 5]. OS is considered a critical factor that causes peroxidation of unsaturated lipids, leading to damage to cell membranes and normal functions [6]. Oxidative damage is often accompanied by an inflammatory reaction [7, 8]. Numerous studies have supported a causal association between NAFLD and higher risk of developing polycystic ovary syndrome [9, 10], and NAFLD has a novel link with reproductive aging by mediating antimüllerian hormone [11]. These studies have reported that OS is the key factor in pathogenesis of disease and aging in liver and ovary [12, 13]. OS associated with FLHS has a negative effect on follicle development, oocyte maturation, and ovulation [14]. The study has shown that alleviating follicle atresia induced by OS can maintain the laying performance of aging laying hens [15]. Fundamentally, the functional integrity of liver and ovaries are closely associated with egg production [16].

Forkhead box class O (FoxO) family comprises FoxO1, FoxO3, FoxO4, and FoxO6 [17]. FoxOs transcription factors primarily regulate stress-response genes to protect organisms from the damage of excessive oxidant stress [18, 19]. FoxOs proteins both regulate and are regulated by OS [20]. They upregulate manganese superoxide dismutase (MnSOD) and response to oxidative DNA damage to protect against oxidative injury [21, 22]. Toll-like receptors (TLRs) play a crucial role in driving cellular inflammatory response and host defense. Inflammatory factors induce TLRs activation, especially *TLR-4* [23]. The role of nuclear factor kappa B (NF-κB) in inflammation and immune response is indisputable, and *NF-κB* can be activated by cellular stress and DNA damage [24]. Additionally, *NF-κB* plays a critical role in promoting adaption to metabolic stress [25]. The *TLR-4/NF-κB* pathway is activated during inflammation development and inhibited during anti-inflammation processed [26]. Pal et al. suggested that *FoxO1* activation and *NF-κB* reduction were the markers of anti-oxidant and anti-inflammation in the ovary [27]. However, the role of the *FoxO*/*TLR-4*/*NF-κB* signaling pathway in regulating OS and inflammation in FLHS has been poorly documented.

Probiotics have been reported to have antioxidative enzyme systems that repair oxidative damage [28], such as $O_2$-consuming enzymes [29], antioxidant enzymes [30], etc. *Lactiplantibacillus plantarum* (*Lp. plantarum*), a type of probiotic, has demonstrated efficacy in alleviating fatty liver disease induced by high-fat diet [31, 32]. *Lp. plantarum* could inhibit *LPS*/*NF-κB* inflammation-related pathway and regulate *PI3K/AKT* pathway to reduce NAFLD [33]. Another research showed that *Lp. plantarum* ameliorates nonalcoholic steatohepatitis-related inflammation by upregulating *L*-arginine production [32]. Meanwhile, numerous studies suggested that *Lp. plantarum* demonstrated the efficiency in enhancing antioxidative capacity and anti-inflammatory effects in chickens [34–36]. These results indicate that *Lp. plantarum* has the potential to relieve OS and inflammation associated with FLHS in laying hens.

So far, the high-energy low-protein (HELP) diet has been developed as the most popular method for establishing a FLHS model [37, 38]. Our previous study established a FLHS laying hen model using a HELP diet, and found that *Lp. plantarum* FRT4 could prevent FLHS by regulating lipid metabolism [39]. These results suggest that *Lp. plantarum* FRT4 has the potential to repair OS in FLHS. Therefore, this study aimed to investigate the mechanisms by which *Lp. plantarum* FRT4 alleviate OS and inflammation in FLHS in laying hens, thereby providing evidence for its application in alleviating OS in laying hens.

## Materials and methods

### Ethics statement

Generated Statement: The animal study was reviewed and approved by the Institutional Animal Care and Use Committee of the Institute of Feed Research of Chinese Academy of Agricultural Sciences (IFR-CAAS20220729).

### Experimental design and animal management

The experimental design and animal management referred to our previous study [39]. Briefly, 450 Hyline brown laying hens aged 44-week were selected and randomly assigned to five groups according to the initial egg laying rate of 80.27%: normal diet (CT, control group), high-energy low-protein diet (HELP, model group), HELP diet supplemented with $10^9$ CFU/kg *Lp.*

*plantarum* FRT4 (FRT4L group, low-dose *Lp. plantarum* FRT4 group), HELP diet with $10^{10}$ CFU/kg *Lp. plantarum* FRT4 (FRT4M group, middle-dose *Lp. plantarum* FRT4 group), and HELP diet with $10^{11}$ CFU/kg *Lp. plantarum* FRT4 (FRT4H group, high-dose *Lp. plantarum* FRT4 group). There were six replications in each group, with 15 hens in each replication. During the trial period, laying hens were housed in a fully enclosed chicken house with a three-story ladder cage system at 65% relative humidity and had free access to water and diet. Following two weeks of normal diet, an eight-week trial was conducted.

The composition and nutrition contents of the normal diet met the NRC (1994) [40], and the composition and nutrition contents of the HELP diet were shown in Additional file 1: Table S1.

#### Sample collection

After fasting 12 h, one laying hen per replicate was randomly selected for sampling at the end of the 8th-week. To collect samples, laying hens were euthanized by cutting their jugular veins.

For the analysis of biochemical parameters and RNA extraction, hepatic and ovarian tissues were collected, snap-frozen immediately, and stored in liquid nitrogen. The caecal content was collected on ice immediately and frozen in liquid nitrogen for subsequent metabolic and metagenomic analysis.

#### Biochemical analysis

Liver or ovarian tissues (0.1 g) were homogenized in 0.9 mL of ice-cold phosphate buffered saline (PBS, pH7.4) using a homogenizer. Then, the homogenates were centrifuged for 15 min at 4°C using a centrifuge at 3,000 × *g* (CT15RE, Hirachi Koki Co., Ltd. Tokyo, Japan). The supernatants were harvested for the determination of biochemistry parameters.

The levels of total anti-oxidation capacity (T-AOC), total superoxide dismutase (T-SOD), catalase (CAT), and glutathione peroxidase (GSH-Px) in liver and ovary were conducted using the kits (catalogue no. A015-2–1, A001-1, A007-1–1, A005-1, respectively) provided by Nanjing Jiancheng Bioengineering Institute (Nanjing, China). The levels of malondialdehyde (MDA), aspartate aminotransferase (AST), and alanine aminotransferase (ALT) in liver and ovary were measured according to the corresponding kits (catalogue no. ml132458, ml092714, and ml092635, respectively). The determination methods were referred to the kits' directions.

The levels of interleukin-1β (IL-1β), IL-6, IL-8, tumor necrosis factor α (TNF-α), NLR family pyrin domain containing 3 (NLRP3), estradiol ($E_2$), follicle stimulating hormone (FSH), and vitellogenin (VTG) in liver and ovary were determined with the corresponding kits (catalogue no. YJ002787, YJ042757, YJ059840, YJ002790, YJ931410, YJ023194, YJ042764, and YJ025401, respectively) provided by Shanghai Enzyme-linked Biotechnology Co., Ltd. (Shanghai, China). All operations were carried out in accordance with the kits' instructions.

#### qRT-PCR analysis

FastPure® Cell/Tissue Total RNA Isolation Kit V2 (RC112-01, Vazyme Biotech Co., Ltd., Nanjing, China) was used for total RNA isolation from hepatic and ovarian tissues. Then, 0.1 μg RNA was used for reverse transcription by using Hiscript® RT SuperMix for qPCR (+gDNA wiper) kits (R323-01, Vazyme Biotech Co., Ltd., Nanjing, China). The reverse productions were used to perform qRT-PCR using the kits of Taq Pro Universal SYBR qPCR Master Mix (Q712-03, Vazyme Biotech Co., Ltd., Nanjing, China). *β-actin* as the house keeping gene was assessed for the stability of expression. The expression level of each gene was calculated by using the $2^{-\Delta\Delta Ct}$ method. The primer sequences for all genes are presented in Additional file 1: Table S2.

#### Untargeted caecal content metabolic analysis with LC-MS and GC-MS

The methods of LC-MS and GC-MS were performed according to our previous study [39].

##### *Caecal content metabolites extraction*

In each of the two replications, 30 mg samples were weighted accurately into EP tubes. Two small steel balls and 600 μL methanol (A452, Thermo Fisher Scientific, Waltham, MA, USA, USA)—water (Wahaha, China) (V: V = 4: 1, containing *L*−2-chlorophenylalanine (C2001, Shanghai Hengchuang Bio-technology Co., Ltd, Shanghai, China, 4 μg/mL) were then put into each tube. The mixture was pre-cooled at − 40°C for 2 min, then placed in a grinder (F-060SD, Fuyang Technology Co., Ltd., Shenzhen, China) for grinding at 60 Hz for 2 min before ultrasonic extraction.

Sample pretreatment for LC-MS method: After ultrasonic extraction in ice water for 10 min, the metabolites were stewed at − 40°C for 2 h. Subsequently, a centrifuge (TGL-16MS, Luxiangyi Centrifuge Instrument Co., Ltd., Shanghai, China) was used to centrifuge the mixed solution at 12,000 × *g* for 10 min at 4°C, followed by filtering 150 μL of supernatant with a 0.22 μm organic phase pinhole filter. For LC–MS analysis, the filtrate was stored at − 80°C. To prepare quality control (QC) samples, the extraction solutions of each sample were mixed in equal volumes.

Sample pretreatment for GC-MS method: After ultrasonic extraction in ice water for 30 min, the metabolites were stewed at − 40°C for 30 min. Subsequently,

a centrifuged solution of 150 μL was gathered into a glass derivative bottle and evaporated using a centrifugal concentration dryer using a centrifugal concentrator (LNG-T98, Huamei Biochemical Instrument Factory, Taicang, China) at 12,000 × *g* for 10 min at 4°C. A 15 mg/mL solution of methoxylamine hydrochloride solution (80 μL) (M813479, Macklin, Shanghai, China)-pyridine (P141169, Aladdin, Shanghai, China) was added to the glass derivative vial, and the mixed solution conduct oximation reaction at 37°C for 60 min in a shaking incubator (THZ-82, Lichen Bangxi Instrument Technology Co., Ltd., Shanghai). After that, the reaction solution was associated with 50 μL BSTFA derivatization reagent (B0830, TCI, Japan), 20 μL N-hexane (4.011518.0500, CNW, Germany), and 10 μL per internal standard (C8/C9/C10/C12/C14/C16/C18/C20/C22/C24, configured with chloroform, G75915B, Greagent, Shanghai, China) to further reaction at 70°C maintained for 60 min, and then the sample was held at room temperature for 30 min. To prepare QC samples, the extraction solutions of each sample were mixed in equal volumes.

#### *LC-MS and GC-MS metabolomic analysis*

LC-MS analysis conditions: For metabolic profiling in both electrospray ionization (ESI) positive and ESI negative modes (Thermo Fisher Scientific, Waltham, MA, USA), a Dionex Ultimate 3000 RS UHPLC was used, equipped with a Q-Exactive plus quadrupole-Orbitrap mass spectrometer. An ACQUITY UPLC HSS T3 column (1.8 μm, 2.1 × 100 mm) were employed in both positive and negative modes. The binary gradient elution system consisted of (A) water (containing 0.1% formic acid, v/v) and (B) acetonitrile and the separation progress was shown in Additional file 1: Table S3. The flow rate was 0.35 mL/min, and column temperature was 45°C. All the samples were kept at 4°C during the analysis. The sample size was 5 μL. The mass spectrometry parameters were shown in Additional file 1: Table S4. Throughout the analysis, QC periodically injected to provide a set of data from which reproducibility could be assessed.

GC–MS analysis conditions: The derivatived samples were analyzed on an Agilent 7890B gas chromatography system coupled to an Agilent 5977 AMSD system (Agilent Technologies Inc., CA, USA) with a DB-5MS capillary column (30 m × 0.25 mm × 0.25 μm, Agilent J & W Scientific, Folsom, CA, USA). High purity helium (> 99.999%) was used as the carrier gas, and the flow rate was 1 mL/min. The temperature of injector was maintained at 260°C. The sample size was 1 μL. The temperature of MS quadrupole was set to 150°C, and the temperature of electron impact ion source was set to 230°C. The collision energy was 70 eV. Mass spectrometric data was acquired in a full-scan mode and the mass scan range was *m/z* 50–500. Throughout the analysis, QC periodically injected to provide a set of data from which reproducibility could be assessed.

#### *Data preprocessing and statistical analysis*

LC-MS method: Progenesis QIV2.3 (Nonlinear Dynamics, Newcastle, UK) was used to process the original LC–MS data for baseline filtering, peak identification, integral, retention time correction, peak alignment, and normalization. The identification of compounds is based on precise *m/z*, secondary fragments, and isotopic distribution, and qualitative analysis is conducted using the Human Metabolomics Database (HMDB), Lipid maps (V2.3), Metlin, EMDB, and PMDB. Then, the extracted data is further processed by removing any peaks with missing values exceeding 50% (ion strength = 0) from the group, replacing zero values with half of the minimum value, and screening based on the qualitative results of the compounds. Compounds with scores below 36 out of 60 were also considered inaccurate and removed. The positive ion data and negative ion data were combined into a data matrix.

GC–MS method: The obtained GC–MS raw data in.D format were transferred to.abf format via software Analysis Base File Converter for quick retrieval of data. Then, data were performed speak detection, peak identification, MS2Dec deconvolution, characterization, peak alignment, wave filtering, and missing value interpolation using software MS-DIAL. After the data was normalized, redundancy removal and peak merging were conducted to obtain the data matrix.

The differential metabolites were distinguished by Orthogonal Partial Least-Squares-Discriminant Analysis (OPLS-DA). sevenfold cross-validation and 200 Response Permutation Testing were used to evaluate the quality of the model and prevent overfitting. Variable Importance of Projection (VIP) values were used to rank the overall contribution of each variable to group discrimination. The significant difference of metabolites between groups was performed by Student's *t*-test. Differential metabolites were selected with VIP values > 1.0 and *P*-values < 0.05.

### Metagenomic analysis of gut microbiota

#### *DNA extraction*

The DNA extraction was performed according to the kit (DP705, Tiangen Biochemical Technology Co., Ltd, Beijing, China). Briefly, 0.25 g samples were added into 2 mL tube, and 500 μL SA and 100 μL SC buffer solutions were added. Meanwhile, 8 pieces with 3 mm and 0.1 g with 1 mm steel balls were added. Then, they were mixed by a grinder (OSE-TH-01, Tiangen) with a condition:

oscillating for 20 s, interval for 10 s, and 2 cycles. After mixed, the mixed solution was split for 15 min with 70°C. The mixed solution was centrifuged for 1 min with 13,400 × *g*. The supernatant (500 μL) was transferred into a new 2 mL tube, and mixed with 200 μL SH buffer solution for eddying 5 s. After stewing for 10 min at 4°C, they were centrifuged 2 min with 13,400 × *g* at a room temperature. Finally, the DNA extraction was performed by a TGuide S96 procedure.

#### *Library construction and sequencing*

Library construction was performed according to a kit (ND617, VAHTS® Universal Plus DNA Library Prep Kit for Illumina). Ten ng DNA was added into 96-well plate, and the volume was up to 17.5 μL with nuclease-free water. After mixed, 2.5 μL FEA buffer and 5 μL FEA enzyme mix were added and mixed. Immediately, the reaction was performed using a PCR instrument (eppendorf6333, Eppendorf). The enzyme digestion interruption was performed with a procedure: 4°C for 15 s, 37°C for 8 min, 65°C for 30 min. The product was connected with a DNA adapter, and then purified with magnetic beads (N411-01, VAHTSTM DNA Clean Beads). Next, the PCR rection was performed for purifying product with PCR primer mix 3 and VAHTS HiFi amplification mix, and the procedure was 95°C for 3 min, 98°C for 20 s, 60°C for 15 s, 72°C for 30, 72°C for 5 min, and lasted for 10 cycles. Subsequently, the PCR product was purified with magnetic beads. Finally, the library quality inspection was performed through Qsep-400, and the library concentration was quantified by Qubit 3.0. For the constructed library, IlluminaNovassq6000 sequencing platform was using for sequencing by paired-end.

#### *Bioinformatic analysis*

The raw reads were quality controlled to obtain clean reads using Trimmomatic software (v0.33): PE LEADING: 3, TRAILING: 3, SLIDINGWINDOW: 50:20, MINLEN:120. The host genome was eliminated using bowtie2 (v2.2.4): seed 123,456-I 200-X 1000-un-conc. The metagenome assemble was performed by MEGAHIT software, and the conting reads were filtrated. Then, the quality estimate to assemble results was using QUAST (v2.3). The MetaGeneMark (http://exon.gatech.edu/meta_gmhmmp.cgi, v 3.26) was using to identify coding regions, and the MMseq2 software (https://github.com/soedinglab/mmseqs2, v 11-e1a1c) was using to remove redundant sequences: similarity 95% and coverage 90%. After that, the non-redundant (Nr) gene sequences were constructed by aligning with Nr database to identify the most similar sequences, and the corresponding annotation information was the Nr gene sequences information. Based on KEGG (Kyoto Encyclopedia of Genes and Genomes) database, the non-redundant sequences were blast and annotated for pathways and KO (KEGG Orthology) terms by Diamond (v0.9.29) with a e-value cutoff of $1e^{-5}$. The non-redundant sequences were blast and annotated to the eggNOG database by Diamond (v0.9.29) with a e-value cutoff of $1e^{-5}$. The hmmer software (v3.0) was used to blast and annotate with Carbohydrate-active enzymes database (CAZy) with if alignment > 80 aa, use e-value < $1e^{-5}$, otherwise use e-value < $1e^{-3}$; covered fraction of HMM > 0.3. The CARD (Comprehensive Antibiotic Research Database) annotation was performed using rgi software (v4.2.2).

#### Statistical analysis

The data were arranged using Excel (version 2019). The differences between two groups were analyzed by *t*-test of SPSS (version 25.0). The graphs were performed using GraphPad Prism version 8.0 (GraphPad Software, San Diego, CA, USA) and expressed as the mean ± SEM, $n = 6$ hens per group. $P < 0.05$ was considered to be significant difference.

According to Nr database annotation results, the microbiota composition and relative abundance were obtained. Taxonomic and functional data analyses were performed by the BMKCloud (https://international.biocloud.net/). The α-diversity and β-diversity were performed with MOTHUR (v.1.35.0) and R package (R ade 4 package, v 2.15.3), respectively. The difference of gene function and microbiota relative abundance was using Kruskal–Wallis test, and $P < 0.05$ was considered significant difference. The correlation of microbiota with biochemical parameters and metabolites was performed using spearman analysis, and $P < 0.05$ was considered significant difference.

## Results

### Effect of *Lp. plantarum* FRT4 on antioxidant capacity and inflammation in liver of laying hens

Supplementation with *Lp. plantarum* FRT4 enhanced the antioxidant capacity in the liver of laying hens (Fig. 1A). Compared to the HELP group, the T-AOC level in the liver of FRT4 groups was significantly increased ($P < 0.05$). The values of T-SOD of liver in the FRT4M and FRT4H groups were higher than that in the HELP group ($P < 0.05$). Meanwhile, the value of GSH-Px in the FRT4H group was higher than that in the HELP group ($P < 0.05$). The contents of MDA, ALT, and AST were significantly increased in the HELP group compared to the CT group ($P < 0.05$), while the contents of MDA and ALT were significantly reduced in the FRT4M and FRT4H groups compared to the HELP group ($P < 0.05$). In addition, the mRNA expression levels of *SOD1*, *SOD2*, *CAT*, and *GPX1* in the FRT4M and FRT4H groups were higher than those

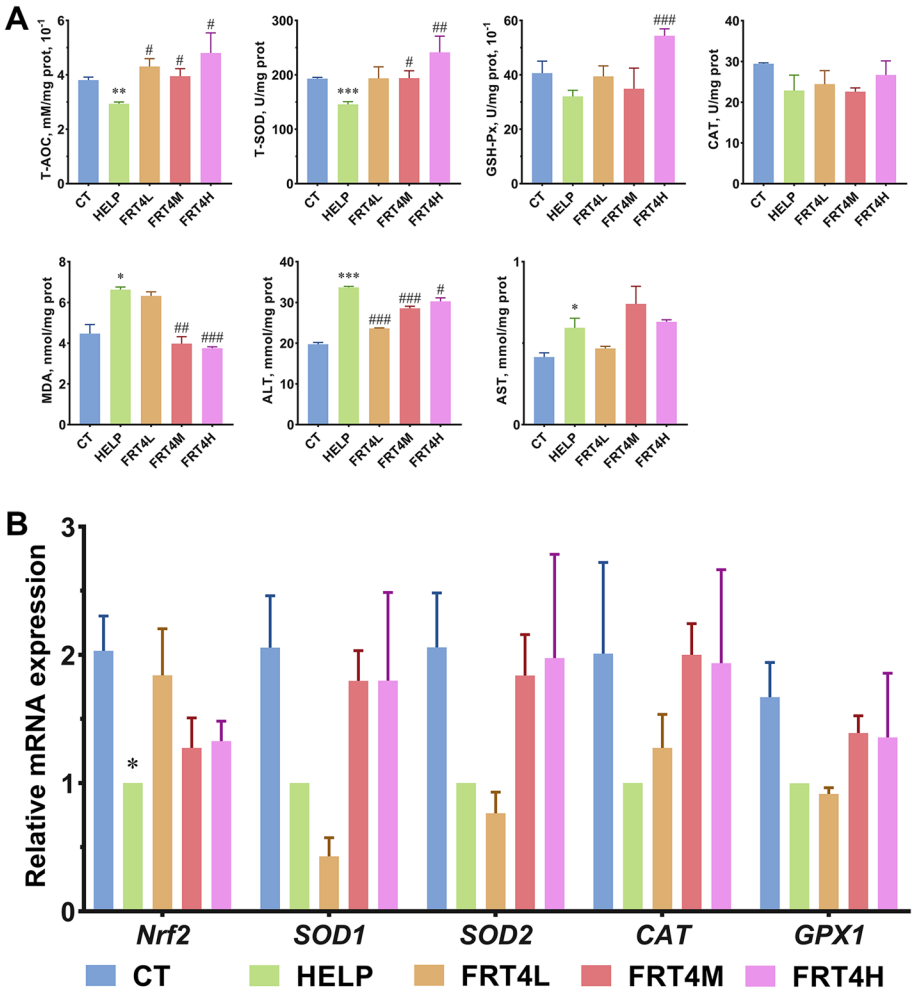


**Fig. 1** Effect of *Lp. plantarum* FRT4 on the antioxidant capacity in the liver of laying hens. **A** The biochemical parameters of antioxidant enzymes in the liver. **B** The relative mRNA expression levels of antioxidant-related factors in the liver. The results were expressed as mean ± SEM, $n = 6$ hens per group. * indicates significant difference between the HELP group and CT groups, and * indicates $P < 0.05$, ** indicates $P < 0.01$, *** indicates $P < 0.001$. # indicates the significant difference between the FRT4L, FRT4M, and FRT4H groups and the HELP group, and # indicates $P < 0.05$, ## indicates $P < 0.01$, ### indicates $P < 0.001$. CT: control group, hens fed with normal diet. HELP: model group, hens fed with high-energy low-protein diet. FRT4L, FRT4M, and FRT4H: experimental groups, hens fed with high-energy low-protein diet with $10^9$ CFU/kg, $10^{10}$ CFU/kg, and $10^{11}$ CFU/kg *Lp. plantarum* FRT4, respectively

in the HELP group ($P > 0.05$) (Fig. 1B). No significant difference was observed for the mRNA expression levels of *SOD1*, *SOD2*, *CAT*, and *GPX1* among the FRT4 supplementation groups ($P > 0.05$). Thus, *Lp. plantarum* FRT4 enhanced the antioxidant capacity in liver of laying hens through increasing the activities and mRNA expression levels of antioxidant related-enzymes.

Supplementation with *Lp. plantarum* FRT4 reduced the level of inflammation in the liver of laying hens (Fig. 2A). Compared to the HELP group, the contents of TNF-α, IL-1β, IL-8, and NLRP3 in the FRT4M and FRT4H groups were significantly decreased after *Lp. plantarum* FRT4 supplementation ($P < 0.05$). The content of IL-6 in the FRT4M group was decreased compared to the HELP group ($P < 0.05$). Meanwhile, the mRNA expression level of *IL-1β* was decreased after *Lp. plantarum* FRT4 supplementation ($P < 0.05$) (Fig. 2B). Although no significant difference was observed among groups, supplementation with *Lp. plantarum* FRT4 decreased the mRNA expression levels of *TNF-α*, *IL-8*, and *NLRP3*. Furthermore, the expression level of the anti-inflammatory *IL-10* was significantly increased in the FRT4L group compared to the HELP group ($P < 0.05$). Thus, *Lp. plantarum* FRT4 improved inflammation level in the liver of laying hens through

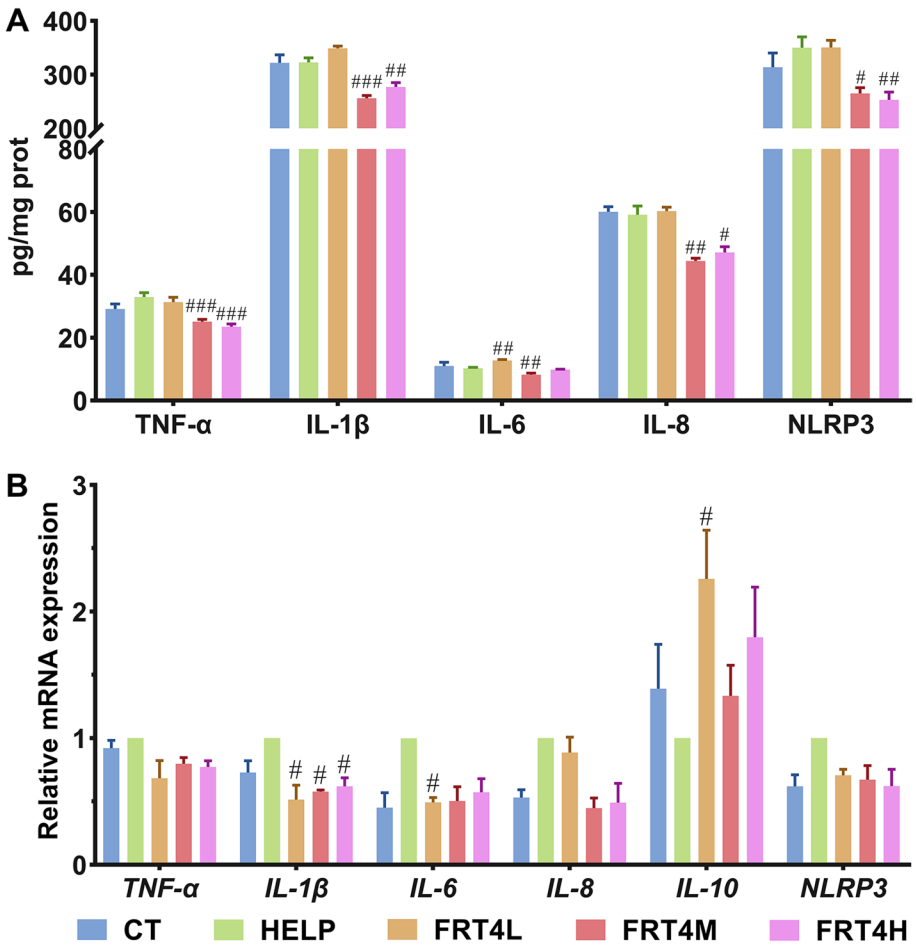


**Fig. 2** Effect of *Lp. plantarum* FRT4 on inflammation in liver of laying hens. **A** The biochemical parameters of inflammatory factors in liver. **B** The relative mRNA expression level of inflammatory factors in the liver. The results were expressed as mean ± SEM, $n = 6$ hens per group. # indicates significant difference between the FRT4L, FRT4M, and FRT4H groups and the HELP group, and # indicates $P < 0.05$, ## indicates $P < 0.01$, ### indicates $P < 0.001$. CT: control group, hens fed with normal diet. HELP: model group, hens fed with high-energy low-protein diet. FRT4L, FRT4M, and FRT4H: experimental groups, hens fed with high-energy low-protein diet with $10^9$ CFU/kg, $10^{10}$ CFU/kg, and $10^{11}$ CFU/kg *Lp. plantarum* FRT4, respectively

regulating the contents and the relative mRNA expression levels of inflammatory factors.

### Effect of *Lp. plantarum* FRT4 on antioxidant capacity and inflammation in ovary of laying hens

The antioxidant capacity was also determined in the ovary of laying hens (Fig. 3A). The T-AOC was increased in groups supplemented with *Lp. plantarum* FRT4, with a significant increase in the FRT4L group ($P < 0.05$). The contents of T-SOD and GSH-Px were significantly increased in the FRT4L group ($P < 0.05$), while the contents of T-SOD and CAT were significantly increased in the FRT4H group ($P < 0.05$). The contents of MDA, ALT, and AST were significantly increased in the HELP group compared to the CT group ($P < 0.05$). Compared to the HELP group, supplementation with *Lp. plantarum* FRT4 significantly reduced the content of ALT and MDA in the FRT4M and FRT4H groups, and the content of AST in the FRT4L group was significantly decreased ($P < 0.05$). Additionally, supplementation with *Lp. plantarum* FRT4 significantly upregulated the mRNA expression level of antioxidant related-factors (Fig. 3B). The mRNA expression levels of *SOD1*, *SOD2*, *GPX1*, and *CAT* were significantly increased in the FRT4M group ($P < 0.05$). The mRNA expression levels of *SOD2*, *GPX1*, and *CAT* were significantly increased in the FRT4L group ($P < 0.05$). Therefore, *Lp. plantarum* FRT4 enhanced the antioxidant capacity in the ovary of laying hens through increasing the activities and mRNA expression levels of antioxidant related-enzymes.

The inflammatory level was determined in the ovary of laying hens (Fig. 4A). Compared to the HELP group, the contents of TNF-α, IL-1β, IL-6, IL-8, and NLRP3 were significantly decreased in the FRT4M group ($P < 0.05$), and the

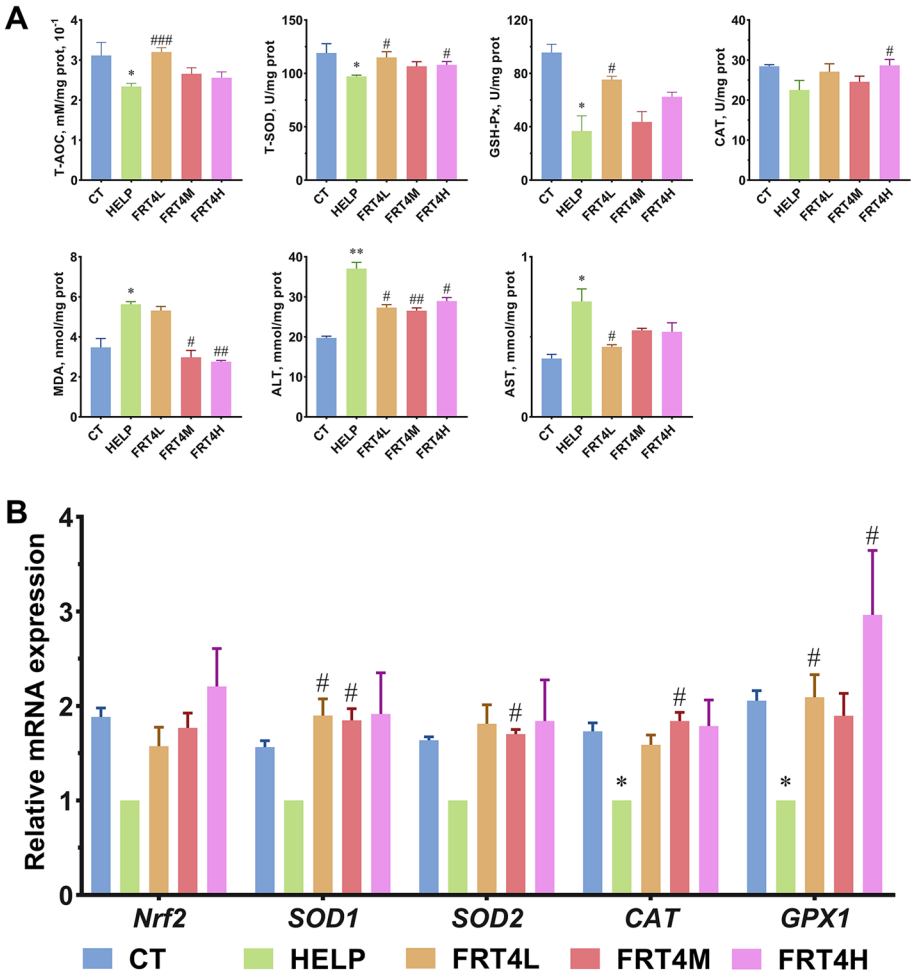


**Fig. 3** Effect of *Lp. plantarum* FRT4 on the antioxidant capacity in ovary of laying hens. **A** The biochemical parameters of antioxidant in ovary. **B** The relative mRNA expression level of antioxidant-related factors in the ovary. The results were expressed as mean ± SEM, $n = 6$ hens per group. * indicates significant difference between HELP group and CT group, and * indicates $P < 0.05$, ** indicates $P < 0.01$. # indicates the significant difference of FRT4L, FRT4M, and FRT4H groups compared to HELP group, and # indicates $P < 0.05$, ## indicates $P < 0.01$, ### indicates $P < 0.001$. CT: control group, hens fed with normal diet. HELP: model group, hens fed with high-energy low-protein diet. FRT4L, FRT4M, and FRT4H: experimental groups, hens fed with high-energy low-protein diet with $10^9$ CFU/kg, $10^{10}$ CFU/kg, and $10^{11}$ CFU/kg *Lp. plantarum* FRT4, respectively

contents of TNF-α, IL-1β, and IL-6 were also significantly decreased in the FRT4H group ($P < 0.05$). Strangely, the contents of TNF-α and NLRP3 were significantly increased in the FRT4L group compared to the HELP group ($P < 0.05$). The mRNA expression levels of *IL-6* and *NLRP3* were significantly decreased in the FRT4M and FRT4H groups compared to the HELP group ($P < 0.05$) (Fig. 4B). The mRNA expression level of *IL-10* was significantly increased in the FRT4L and FRT4M groups compared to the HELP group ($P < 0.05$). Thus, *Lp. plantarum* FRT4 improved the inflammation level in the ovary of laying hens through regulating the contents and the mRNA expression of inflammatory factors.

## Effect of *Lp. plantarum* FRT4 on caecal content metabolites through untargeted metabonomics analysis

### *Multivariate statistical analysis of caecal content metabolites*

After quality control, in order to display the classification of metabolites more intuitively, the Pie charts were used to show the categories of caecal content metabolites at the class level (Fig. 5A and B). The top 9 categories with the highest number of metabolites were displayed, and the remaining categories were merged into "others". In LC–MS analysis, the metabolites were identified as benzene and substituted derivatives (5.66%), carboxylic acids and derivatives (11.65%), fatty acyls (15.72%), glycerophospholipids (3.93%), organooxygen compounds (6.32%), polyketides (2.39%), prenol lipids (7.99%), and steroids and steroid derivatives (7.39%). In GC–MS analysis, the metabolites were identified as benzene and

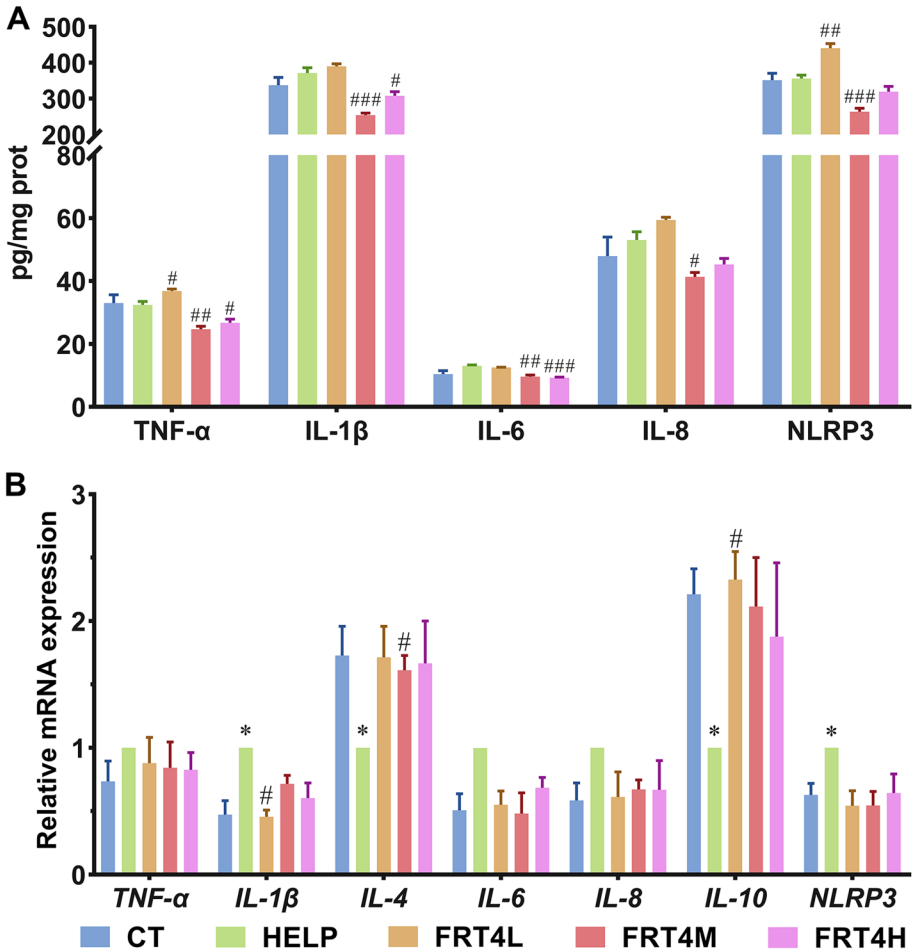


**Fig. 4** Effect of *Lp. plantarum* FRT4 on inflammation in the ovary in laying hens. **A** The biochemical parameters of inflammatory factors in ovary. **B** The relative mRNA expression level of inflammatory-related factors in the ovary. The results were expressed as mean ± SEM, $n = 6$ hens per group. * indicates the significant difference of HELP group compared to CT group, and * indicates $P < 0.05$. # indicates the significant difference of FRT4L, FRT4M, and FRT4H groups compared to HELP group, and # indicates $P < 0.05$, ## indicates $P < 0.01$, ### indicates $P < 0.001$. CT: control group, hens fed with normal diet. HELP: model group, hens fed with high-energy low-protein diet. FRT4L, FRT4M, and FRT4H: experimental groups, hens fed with high-energy low-protein diet with $10^9$ CFU/kg, $10^{10}$ CFU/kg, and $10^{11}$ CFU/kg *Lp. plantarum* FRT4, respectively

substituted derivatives (5.19%), carboxylic acids and derivatives (14.32%), fatty acyls (15.35%), glycerolipids (2.28%), hydroxy acids and derivatives (3.11%), organooxygen compounds (20.12%), phenols (2.49%), and steroids and steroid derivatives (4.36%). OPLS-DA was used to determine the metabolites, and a permutation test was conducted to display the stability of the OPLS-DA model. As shown in Fig. 5C-F, the OPLS-DA score scatter plot showed significant differences between the FRT4M group and HELP group, which indicated that *Lp. plantarum* FRT4 changed the caecal content metabolites of laying hens. Additionally, the permutation test displayed the stability of the OPLS-DA model (Fig. 5G-J), indicating that OPLS-DA model had a good quality and was not over-fitted.

### *Differential metabolites analysis*

Based on the OPLA-DA analysis, the VIP was used to measure the influence intensity and interpretation ability of the expression mode of each metabolite on the classification and discrimination. Further *t* test was used to verify whether the different metabolites between two groups were significant. Finally, according to VIP > 1 and $P < 0.05$, 633 differential metabolites were identified in the HELP group compared to the CT group, and 129 differential metabolites were identified in FRT4M group compared to the HELP group (Additional file 2).

Compared to the CT group, 41 differential metabolites involving benzene and substituted derivatives were significantly altered in the HELP group ($P < 0.05$) (Fig. 6A), including bevantolol, hydroxyhexamide, hydroxyzine, 5-aminosalicylic acid, 3-hydroxyanthranilic acid, and

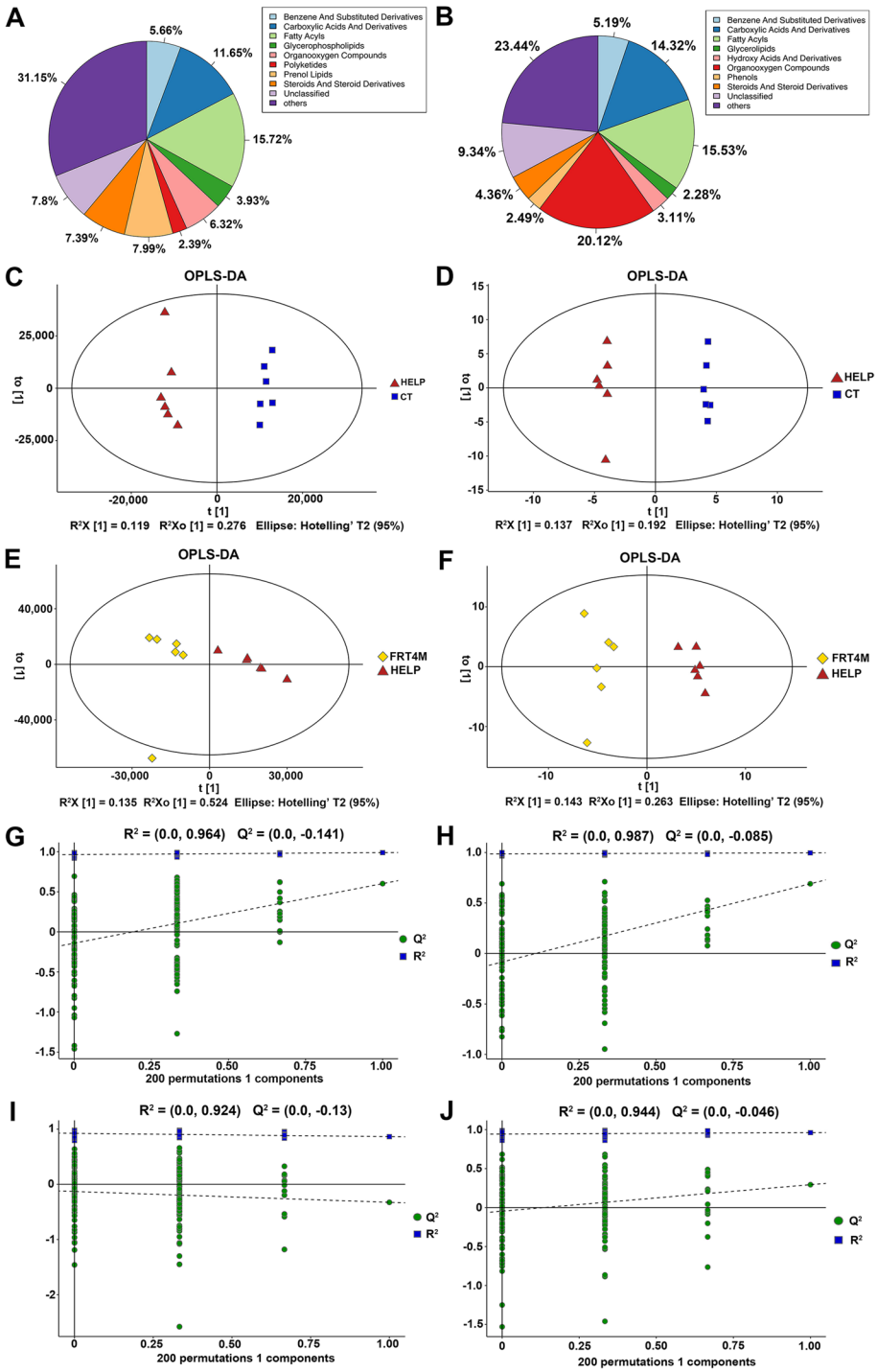


**Fig. 5** The multivariable statistics of caecal content metabolites. **A**, **C**, **E**, **G**, **I** LC-MS. **B**, **D**, **F**, **H**, **J** GC-MS. **A**, **B** The Pie charts of caecal content metabolites. The top 9 categories with the highest number of metabolites were shown, and the other categories were merged into others. **C**, **D** The OPLS-DA score scatter for HELP group compared to the CT group. **E**, **F** The OPLS-DA score scatter for FRT4M group compared to the HELP group. **G**, **H** The permutation test displaying the stability for HELP group compared to the CT group. **I**, **J** The permutation test displaying the stability for FRT4M group compared to the HELP group. CT: control group, hens fed with normal diet. HELP: model group, hens fed with high-energy low-protein diet. FRT4M: experimental groups, hens fed with high-energy low-protein diet with $10^{10}$ CFU/kg *Lp. plantarum* FRT4

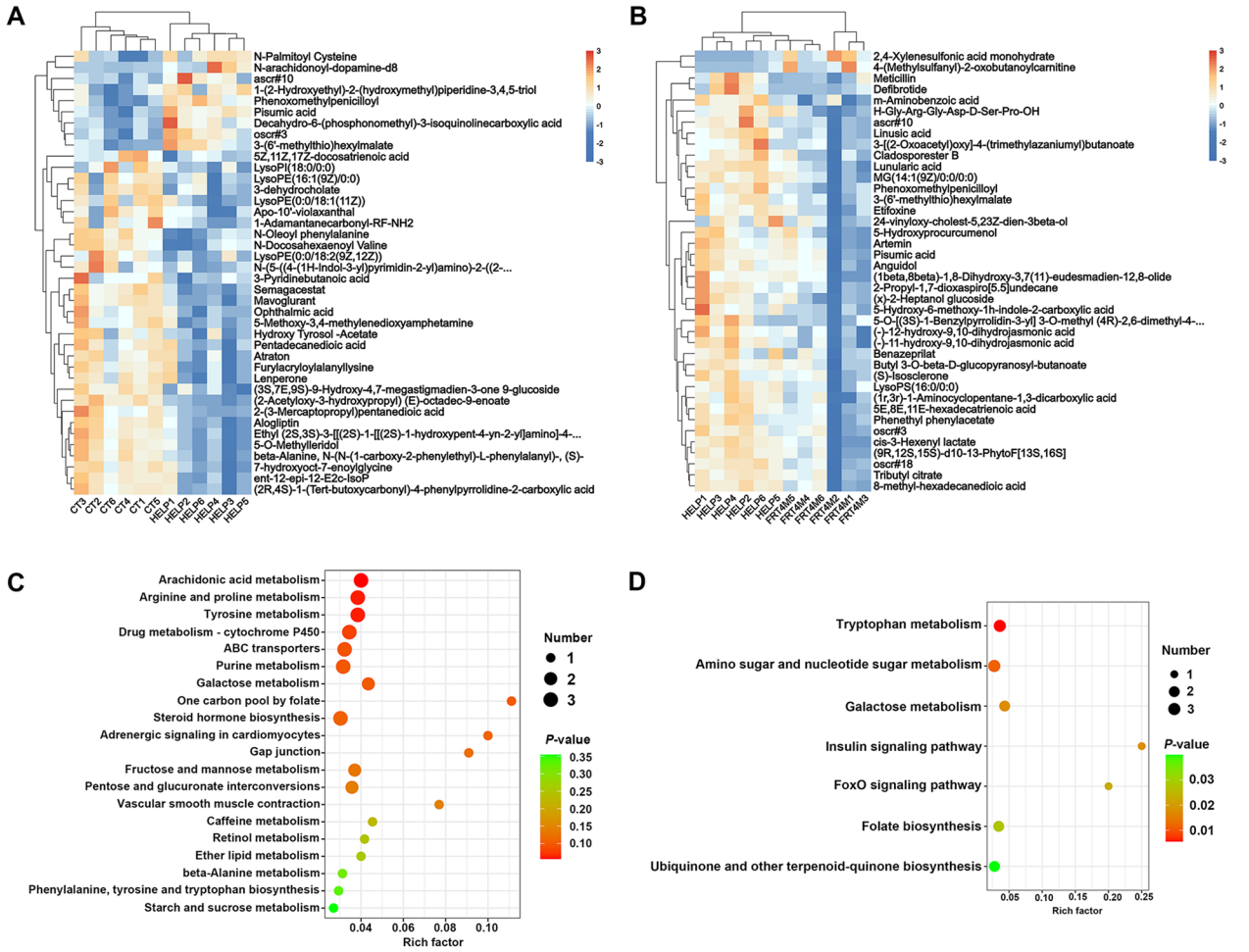


**Fig. 6** Effect of *Lp. plantarum* FRT4 on differential metabolites and metabolism pathways in caecal content of laying hens. **A** The differential metabolites in caecal content for the HELP group compared to the CT group. **B** The differential metabolites in caecal content for the FRT4M group compared to the HELP group. **C** The differential metabolism pathway based on differential metabolites for the HELP group compared to the CT group. **D** The differential metabolism pathway based on differential metabolites for the FRT4M group compared to the HELP group. CT: control group, hens fed with normal diet. HELP: model group, hens fed with high-energy low-protein diet. FRT4M: experimental groups, hens fed with high-energy low-protein diet with $10^{10}$ CFU/kg *Lp. plantarum* FRT4

3-hydroxy-3-phenylpentanamide. Seventy-six differential metabolites involving carboxylic acids and derivatives were significantly ($P<0.05$) changed, including phenoxomethylpenicilloyl, *N*-jasmonoyltyrosine, *L*-agaridoxin, tricarballylic acid, furylacryloylalanyllysine, and ophthalmic acid. Ninety-six differential metabolites involving fatty acyls were significantly altered ($P<0.05$), including leucrose, oscr#3, tetranorprostanedioic acid, pentadecylic acid, tridecylic acid, pentadecanedioic acid. Eighteen differential metabolites involving glycerophospholipids lysoPE(0:0/18:4(6Z,9Z,12Z,15Z)), PI(17:1(9Z)/18:0), PS(13:0/0:0), glycerophosphoric acid, lysoPI(18:0/0:0), and lysoPE(0:0/18:2(9Z,12Z)) were significantly altered ($P<0.05$). Fifty differential metabolites involving steroids and steroid derivatives were significantly altered ($P<0.05$), including trilostane, daturmeteside E, 25-hydroxy-atrotosterone A, coprostanol, 2-methoxyestradiol, and 3-dehydrocholate. Sixty-five differential metabolites involving prenol lipids ($P<0.05$), artemisin, tomenphantin A, 11-deoxoglycyrrhetinic acid, gibberellin A112, gibberellin A43, and dehydrocostus lactone. Forty-nine differential metabolites involving organonitrogen compounds were significantly altered ($P<0.05$), including heptanoylcholine, ethametsulfuron-methyl, digoxigenin monodigitoxoside, pirimicarb, *D*-tagatose, and niazicinin. Twenty-four differential metabolites involving polyketides were significantly altered ($P<0.05$), including calomelanol H, agestricin D, sutchuenoside A, 5-*O*-methylleridol, plagionicin A, and 1-benzylpiperidine-4-carboxylic acid.

Compared to the HELP group, 9 differential metabolites involving benzene and substituted derivatives were significantly altered in the FRT4M group ($P<0.05$) (Fig. 6B), including 2-pyrocatechuic acid, 4-hydroxyphenylpyruvic acid, *p*-aminobenzoic acid, 4-hydroxybenzoic acid, phenethyl phenylacetate, *m*-aminobenzoic acid, nitroflurbiprofen, seladelpar, and *p*-mentha-1,3,5,8-tetraene. Seventeen differential metabolites involving carboxylic acids and derivatives were significantly altered ($P<0.05$), including meticillin, phenoxomethylpenicilloyl, *cis*−3-hexenyl lactate, (1r,3r)−1-aminocyclopentane-1,3-dicarboxylic acid, and pheneticillin. Twenty-seven differential metabolites involving fatty acyls were significantly altered ($P<0.05$), including (-)−11-hydroxy-9,10-dihydrojasmonic acid, (-)−12-hydroxy-9,10-dihydrojasmonic acid, ascr#10, oscr#3, linusic acid, (x)−2-heptanol glucoside, 4-(methylsulfanyl)−2-oxobutanoylcarnitine, butyl 3-o-beta-d-glucopyranosyl-butanoate, and 8-methyl-hexadecanedioic acid. Eleven differential metabolites involving organooxygen compounds were significantly altered ($P<0.05$), including *cis*−4-hydroxycyclohexylacetic acid, *D*-tagatose, daumone, sergliflozin A, and *L*-carnitine. Fifty differential metabolites involving prenol lipids were significantly altered ($P<0.05$), including pisumic acid, 5-hydroxyprocurcumenol, artemin, anguidol, (-)-picrotoxinin, (1β, 8β)−1,8-dihydroxy-3,7(11)-eudesmadien-12,8-olide, ditaxanthin, 3-(4-isopropylphenyl) propanal.

#### *Differential metabolic pathway analysis*

The differential metabolites were analyzed through pathway enrichment analysis based on KEGG database (Additional file 3). There were 30 KEGG pathways identified in the HELP group compared to the CT group (Fig. 6C), including arachidonic acid metabolism, arginine and proline metabolism, tyrosine metabolism, drug metabolism-cytochrome P450, ABC transporters, etc. There were 20 metabolic pathways identified in the FRT4M group compared to the HELP group, including 7 differential metabolic pathways ($P<0.05$) (Fig. 6D). The differential metabolic pathways were tryptophan metabolism, amino sugar and nucleotide sugar metabolism, galactose metabolism, insulin signaling pathway, FoxO signaling pathway, folate biosynthesis, and ubiquinone and other terpenoid-quinone biosynthesis.

### Effect of *Lp. plantarum* FRT4 on the structure and function of gut microbiota in laying hens

#### *Effect of Lp. plantarum FRT4 on gut microbiota structure of laying hens*

Metagenomic analysis was used in this study to analyze the caecal microbiota. At the phylum level (Fig. 7A), the total of relative abundances of Bacteroidetes, Firmicutes, and Proteobacteria was more than 93% in the CT, HELP, and FRT4M groups. Compared to the CT group, the relative abundances of Bacteroidetes, Proteobacteria, and Elusimicrobia were decreased in the HELP group, while the relative abundances of Firmicutes, Synergistetes, and Tenericutes were increased. At the genus level (Fig. 7B), compared to the CT group, the relative abundances of *Bacteroides*, *Phocaeicola*, *Alistipes*, *Prevotella*, *Muribaculum*, *Mediterranea*, and *Parabacteroides* were decreased in the HELP group, while the relative abundances of *Clostridium*, *Faecalibacterium*, and *Lachnoclostridium* were increased. At the species level (Fig. 7C), compared to the CT group, the relative abundances of *Alistipes*_sp._CAG_831, *Phocaeicola_barnesiae*, *Mediterranea*_sp._An20, uncultured_*Bacteroides*_sp., *Bacteroides_togonis*, *Phocaeicola_vulgatus*, and *Bacteroides_ndongoniae* were decreased in the HELP group, while the relative abundances of *Bacteroides*_sp._An322, *Clostridiales_bacterium*, and *Phocaeicola_plebeius* were increased. Furthermore, the nonparameteric test was to analyze the differential taxonomy among groups by Kruskal-Wallis.

In addition, there were 636 differential species taxonomies found among the CT, HELP, and FRT4M groups (Additional file 4). Further, the top 20 dominant differential species among groups were selected to draw the heatmap, which also showed their phylum, family, and genus (Fig. 7D). Compared to the HELP group, the relative abundances of *Clostridium_sp._CAG_1013*, *Anaerotruncus_colihominis*, *Firmicutes_bacterium_CAG_94*, *Agathobaculum_sp._Marseille_P7918*, *Angelakisella_massiliensis*, *Clostridium_sp._CAG_169*, and *uncultured_Clostridium_sp.* were decreased, and the relative abundances of *Alistipes_sp._CAG_514*, *Alistipes_sp._CAG_435*, *Bacteroides_sp._CAG_770*, *Bacteroides_sp._CAG_709*, *Bacteroides_sp._CAG_545*, and *Bacteroidales_bacterium_WCE2008* were increased in the CT and FRT4M groups. These results showed that the gut microbiota structure in laying hens was disordered after feeding the HELP diet. However, these disorders were repaired after *Lp. plantarum* FRT4 supplementation, which made the caecal microbiota structure more similar to that of the CT group.

As shown in Fig. 7E, the simpson index of α-diversity increased in the HELP group compared to the CT group ($P=0.153$), and decreased in the FRT4M group compared to the HELP group ($P=0.023$), while no significant difference was observed between the CT and FRT4M groups ($P=0.302$). The PCA analysis showed no obvious difference among the groups. However, the distance between the CT and FRT4M groups appear to be closer, suggesting a more similar microbial community structure between these two groups (Fig. 7F).

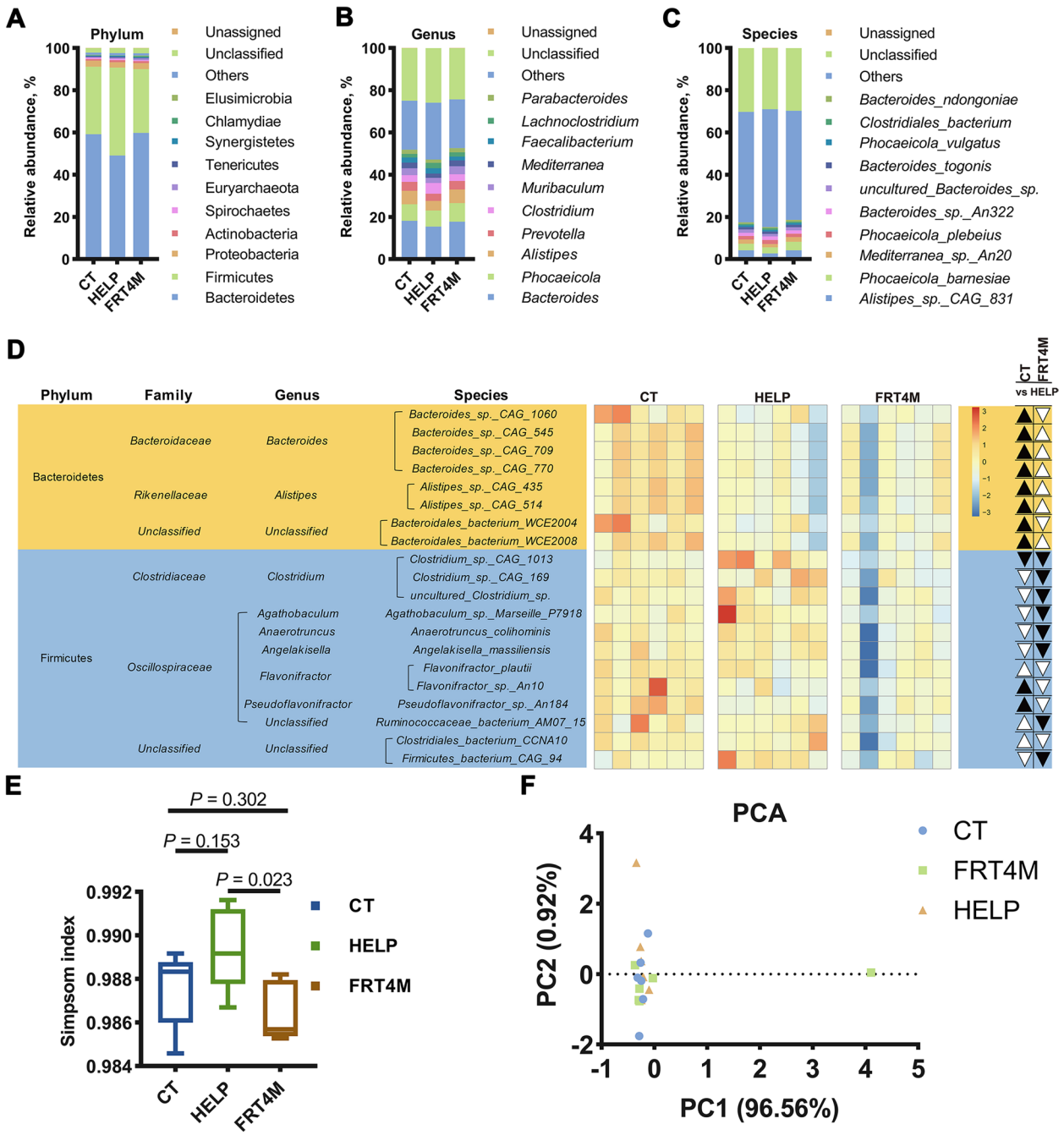


**Fig. 7** The microbiota diversity of caecal content in laying hens. **A** The microbiota structure at the phylum level. **B** The microbiota structure at the genus level. **C** The microbiota structure at the species level. **D** The heat-map of the top 20 dominant differential species among groups. The upward triangle indicates upregulation, and the downward triangle indicates downregulation. The black indicates a significant difference, and white indicates no significant difference. **E** The Simpson index of α-diversity. **F** The PCA analysis of β-diversity based on bray_curtis. CT: control group, hens fed with normal diet. HELP: model group, hens fed with high-energy low-protein diet. FRT4M: experimental groups, hens fed with high-energy low-protein diet with $10^{10}$ CFU/kg *Lp. plantarum* FRT4

### *Effect of Lp. plantarum FRT4 on the function of gut microbiota in laying hens*

Based on the Kruskal–Wallis functional gene difference analysis (Fig. 8), the top 8 differential KEGG pathways were ranked by significance and displayed in descending order of abundance. These pathways included aminobenzoate degradation, beta-alanine metabolism, valine, leucine and isoleucine degradation, lipopolysaccharide biosynthesis,

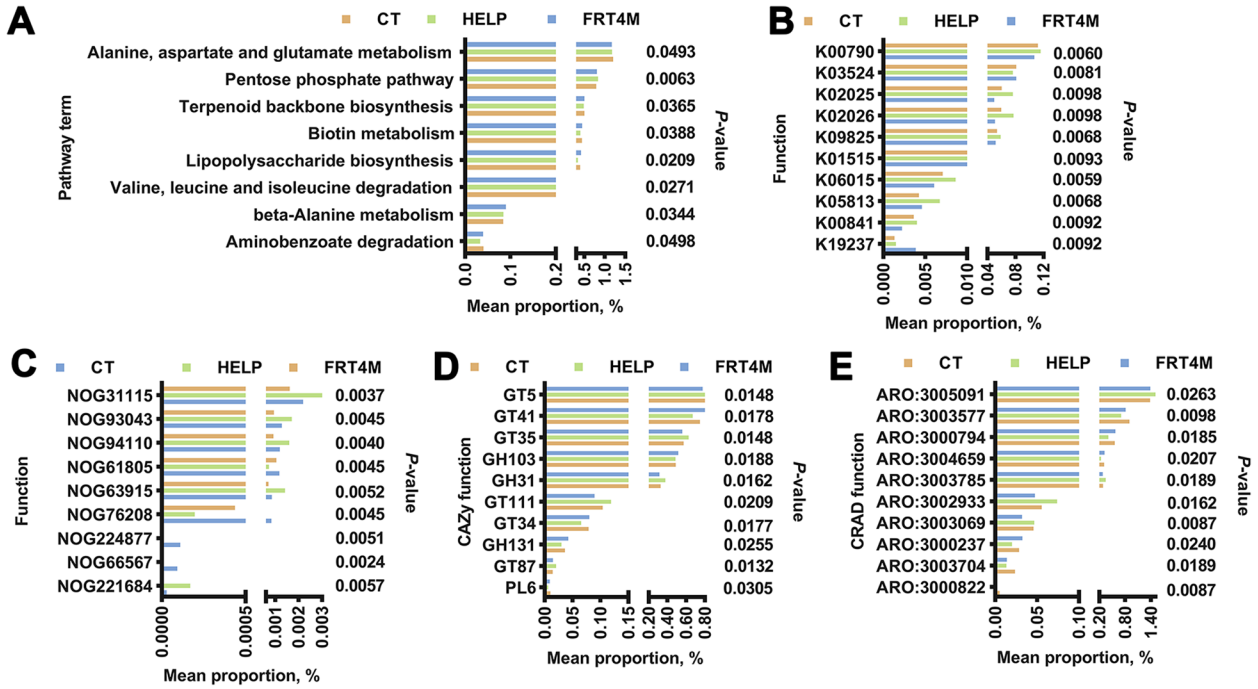


**Fig. 8** The gene function diversity of caecal content microbiota in laying hens. The difference analysis was based on Kruskal-Wallis.**A** The KEGG pathway term enrichment. **B** The KO function. **C** The eggNOG function. **D** The CAZy function. GH: glycoside hydrolases, GT: glycosyl transferases, PL: polysaccharide lyases. **E** The ARO function of CARD. ARO: antibiotic resistance ontology

biotin metabolism, terpenoid backbone biosynthesis, pentose phosphate pathway, and alanine, aspartate and glutamate metabolism (Fig. 8A). The top 10 differential KO functions were K00790, K03524, K02025, K02026, K09825, K01515, K06015, K05813, K00841, and K19237 (Fig. 8B). The top 10 differential eggNOG functions were NOG31115, NOG93043, NOG94110, NOG61805, NOG63915, NOG76208, NOG224877, NOG66567, and NOG221684 (Fig. 8C). The top 10 differential CAZy functions were GT5, GT41, GT35, GH103, GH31, GT111, GT34, GH131, GT87, and PL6 (Fig. 8D). The top 10 differential CARD functions were ARO3005091, ARO3003577, ARO3000794, ARO3004659, ARO3003785, ARO3002933, ARO3003069, ARO3000237, ARO3003704, and ARO3000822 (Fig. 8E).

### *Correlation of caecal microbiota and biochemical parameters of laying hens*

Based on spearman analysis, the correlation between caecal microbiota at different taxonomic levels and biochemical parameters of laying hens are shown in Fig. 9. At the phylum level (Fig. 9A), Bacteroidetes was positively related to GSH-Px and T-SOD ($P<0.05$), and negatively related to TNF-α ($P<0.05$). The Euryarchaeota was negatively related to IL-8 and CAT ($P<0.05$). Firmicutes was positively related to MDA and TNF-α ($P<0.05$), and negatively related to GSH-Px and T-SOD ($P<0.05$). Actinobacteria was positively related to IL-6 ($P<0.05$). At the class level (Fig. 9B), Bacteroidia was positively related to GSH-Px and T-SOD ($P<0.05$), and negatively related to TNF-α ($P<0.05$). Methanobacteria was negatively related to CAT, IL-1β, and IL-8 ($P<0.05$). Coriobacteriia was positively related to IL-6 ($P<0.05$), and negatively related to T-AOC and T-SOD ($P<0.05$). Clostridia was negatively related to GSH-Px and T-SOD ($P<0.05$). Erysipelotrichia was positively related to IL-1β, IL-8, NLRP3, MDA, and TNF-α ($P<0.05$). At the genus level (Fig. 9C), *Clostridium* was negatively related to GSH-Px ($P<0.05$). *Faecalibacterium* was positively related to CAT ($P<0.05$). *Alistipes* was positively related to T-SOD ($P<0.05$), and negatively related to MDA ($P<0.05$). *Bacteroides* was positively related to GSH-Px and T-SOD ($P<0.05$), and negatively related to NLRP3 ($P<0.05$). *Parabacteroides* was negatively related to MDA and TNF-α ($P<0.05$). At the species level (Fig. 9D), *Phocaeicola_barnesiae* was negatively related to NLRP3 ($P<0.05$). The *Alistipes_* sp._CAG_831 was positively related to T-SOD ($P<0.05$). *Phocaeicola_plebeius* was positively related to GSH-Px ($P<0.05$).

### Effect of *Lp. plantarum* FRT4 on *FoxO/TLR-4/NF-κB* signaling pathway related-factors in liver and ovary of laying hens

The effect of *Lp. plantarum* FRT4 on *FoxO/TLR-4/NF-κB* signaling pathway-related factors in the liver is shown in

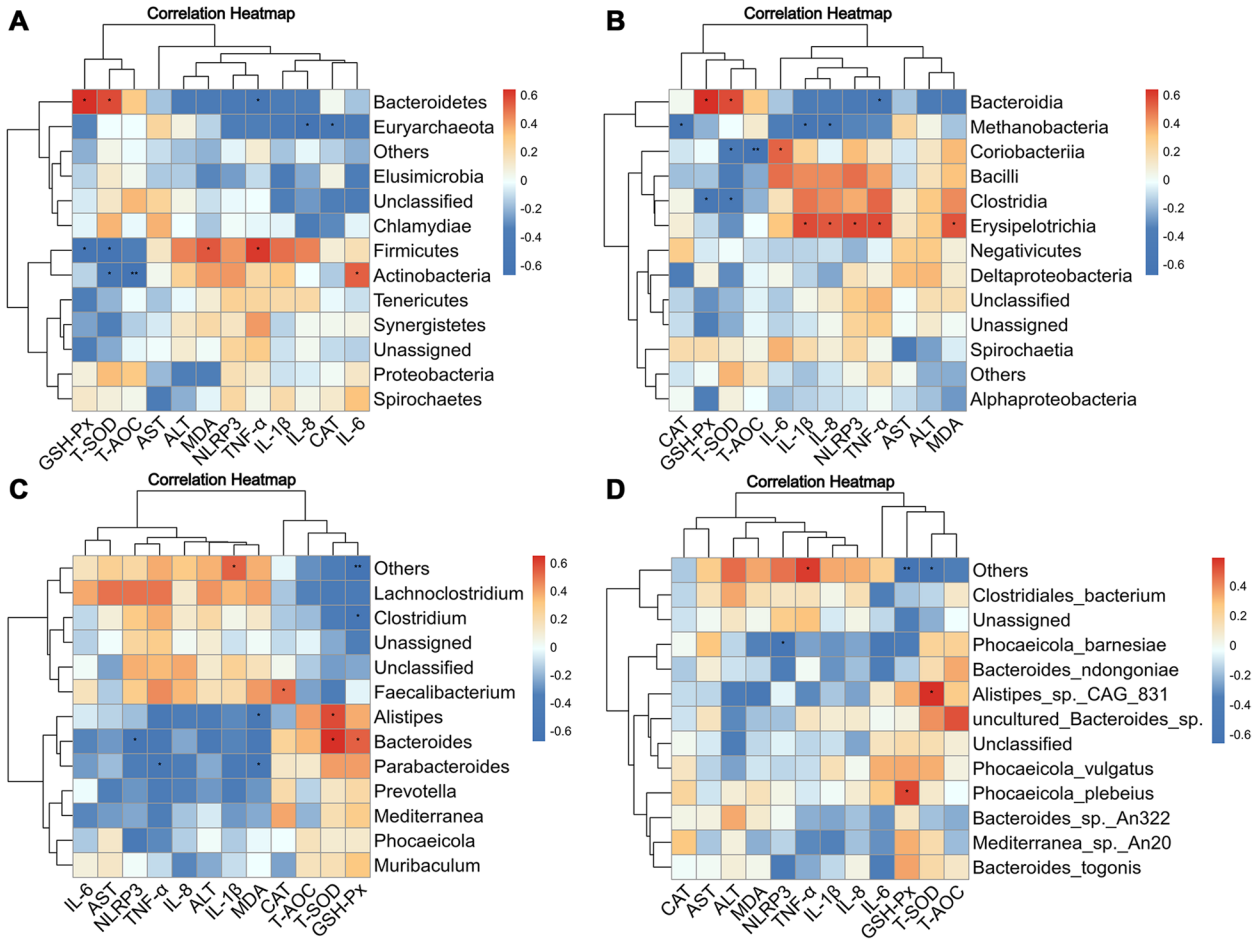


**Fig. 9** The correlation between biochemical parameters and caecal microbiota at different levels. **A** The correlation between liver biochemical parameters and caecal microbiota at the phylum level. **B** The correlation between liver biochemical parameters and caecal microbiota at the class level. **C** The correlation between liver biochemical parameters and caecal microbiota at the genus level. **D** The correlation between liver biochemical parameters and caecal microbiota at the species level. * indicates $P < 0.05$, ** indicates $P < 0.01$

Fig. 10A. Compared to the CT group, the relative mRNA expression level of *TLR-4* was significantly increased in the HELP group ($P < 0.05$), while supplementation with *Lp. plantarum* FRT4 significantly reduced the relative mRNA expression level of *TLR-4* ($P < 0.05$). Compared to the HELP group, the relative mRNA expression level of *NF-κB* was significantly decreased after *Lp. plantarum* FRT4 intervention ($P < 0.05$). Compared to the CT group, the relative mRNA expression level of *FoxO3* was significantly decreased in the HELP group ($P < 0.05$). Compared to the HELP group, the relative mRNA expression level of *FoxO1* was significantly increased in the FRT4L group ($P < 0.05$), with *P*-value of 0.094 between the HELP and FRT4M groups.

The effect of *Lp. plantarum* FRT4 on *FoxO/TLR-4/NF-κB* signaling pathway-related factors in the ovary is shown in Fig. 10B. Compared to the CT, the relative mRNA expression level of *TLR*−4 was significantly increased in HELP group ($P < 0.05$). Compared to the HELP group, the relative mRNA expression level of *TLR-4* was significantly decreased in FRT4L and FRT4M groups ($P < 0.05$). The relative mRNA expression level of *NF-κB* was significantly decreased in the FRT4L group ($P < 0.05$), and the relative mRNA expression level of *FoxO1* was significantly increased in the FRT4M group ($P < 0.05$).

Moreover, the relationship between gut microbiota at the genus level and *FoxO/TLR-4/NF-κB* signaling pathway was analyzed. As shown in Fig. 10C, in the liver, *Bacteroides* and *Parabacteroides* were significantly positively related to *FoxO1*, and negatively related to *NF-κB* ($P < 0.05$). *Bacteroides* was also significantly positively related to *FoxO3* ($P < 0.05$). *Lachnoclostridium* was significantly negatively related to *NF-κB* ($P < 0.05$), and *Mutribaculum* was significantly negatively related to *TLR-4* ($P < 0.05$). However, *Lachnoclostridium* was

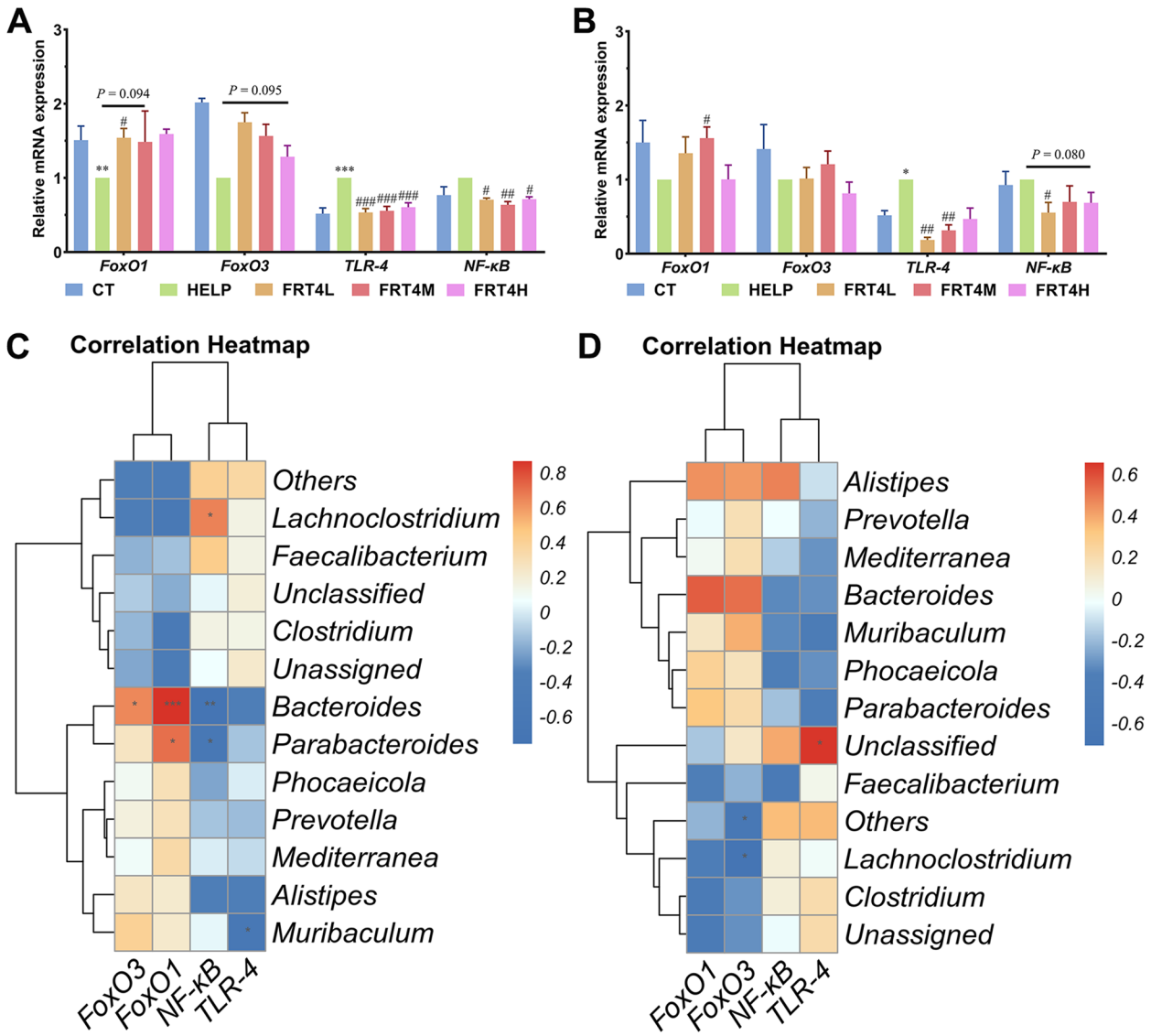


**Fig. 10** Effect of *Lp. plantarum* FRT4 on *FoxO/TLR-4/NF-κB* signaling pathway-related factors in laying hens. **A** Effect of *Lp. plantarum* FRT4 on *FoxO/TLR-4/NF-κB* signaling pathway-related factors in the liver of laying hens. **B** Effect of *Lp. plantarum* FRT4 on *FoxO/TLR-4/NF-κB* signaling pathway-related factors in the ovary of laying hens. **C** The correlation between *FoxO/TLR-4/NF-κB* signaling pathway-related factors in the liver and gut microbiota at the genus level. **D** The correlation between *FoxO/TLR-4/NF-κB* signaling pathway-related factors in the ovary and gut microbiota at the genus level. The results were expressed as mean ± SEM, $n = 6$ hens per group. **A**, **B** * indicates the significant difference between the HELP group and the CT group, and * indicates $P < 0.05$, ** indicates$P < 0.01$, *** indicates $P < 0.001$. # indicates the significant difference between the FRT4L, FRT4M, and FRT4H groups and the HELP group, and # indicates $P < 0.05$, ## indicates $P < 0.01$, ### indicates $P < 0.001$. CT: control group, hens fed with normal diet. HELP: model group, hens fed with high-energy low-protein diet. FRT4L, FRT4M, and FRT4H: experimental groups, hens fed with high-energy low-protein diet with $10^9$ CFU/kg, $10^{10}$ CFU/kg, and $10^{11}$ CFU/kg *Lp. plantarum* FRT4, respectively. **C**, **D** * indicates $P < 0.05$, ** indicates $P < 0.01$, *** indicates$P < 0.001$

significantly negatively related to *FoxO3* in the ovary ($P < 0.05$, Fig. 10D).

Thus, *Lp. plantarum* FRT4 improved the antioxidant capacity and inflammation in the liver and ovary of laying hens by regulating the *FoxO/TLR-4/NF-κB* signaling pathway and gut microbiota.

### Effect of *Lp. plantarum* FRT4 on estrogen of laying hens

*Lp. plantarum* FRT4 can increase the overall level of estrogen in laying hens. As shown in Fig. 11A, the contents of estradiol ($E_2$) and VTG in the FRT4L group in liver were significantly higher than those in the HELP group ($P < 0.05$). In the ovary (Fig. 11B), compared with

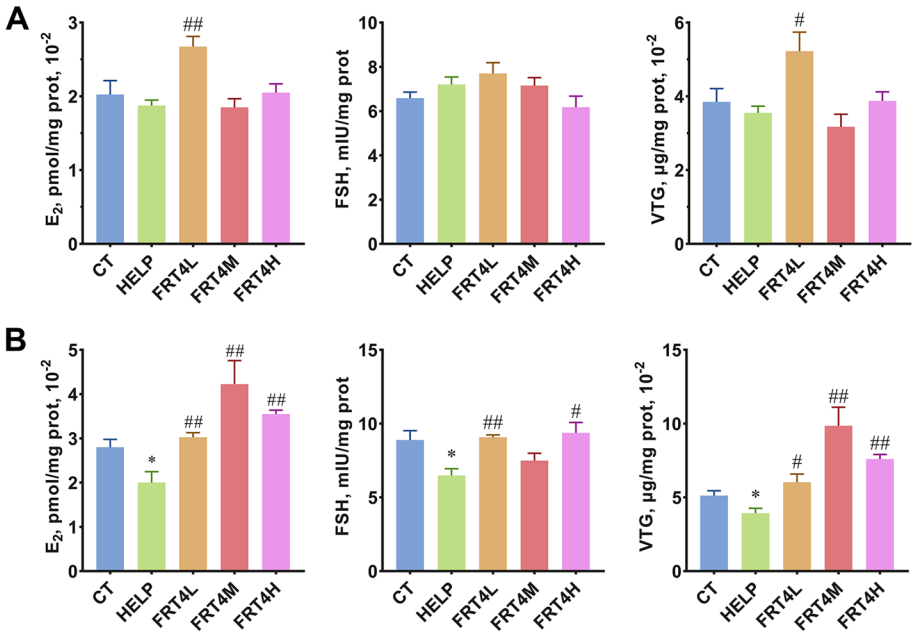


**Fig. 11** Effect of *Lp. plantarum* FRT4 on estrogen in laying hens. **A** The content of estrogen in liver. **B** The content of estrogen in ovary. $E_2$: estradiol, FSH: follicle-stimulating hormone, VTG: vitellogenin. The results were expressed as mean ± SEM, $n = 6$ hens per group. * indicates the significant difference between the HELP group and the CT group, and * indicates $P < 0.05$. # indicates the significant difference between FRT4L, FRT4M, and FRT4H groups and the HELP group, and # indicates $P < 0.05$, ## indicates $P < 0.01$. CT: control group, hens fed with normal diet. HELP: model group, hens fed with high-energy low-protein diet. FRT4L, FRT4M, and FRT4H: experimental groups, hens fed with high-energy low-protein diet with $10^9$ CFU/kg, $10^{10}$ CFU/kg, and $10^{11}$ CFU/kg *Lp. plantarum* FRT4, respectively

the CT group, the levels of $E_2$, follicle-stimulating hormone (FSH), and VTG in the HELP group were significantly reduced ($P < 0.05$). Compared to the HELP group, adding *Lp. plantarum* FRT4 significantly increased $E_2$ and VTG content ($P < 0.05$), and the contents of FSH in FRT4L and FRT4H groups were significantly increased ($P < 0.05$). In addition, the mRNA expression level of estrogen receptor 1 (*ESR1*) in ovary significantly was decreased in the HELP group compared to the CT group ($P < 0.05$) (Fig. 12). Compared to the HELP group, the mRNA expression level of *ESR1* was increased in the FRT4M and FRT4H groups.

## Discussion

FLHS is typically associated with lipid peroxidation, hepatocyte injury, reduced antioxidant capacity, and inflammation [41]. Yuan et al. reported that high-fat diet decreased the hepatic antioxidant capacity of mice [42], and NAFLD would cause liver injury [43, 44]. Previous studies also suggested that HELP diet could limit the hepatic antioxidant capacity of laying hens [38], and increase the inflammation level [45]. In this study, feeding HELP diet significantly decreased the concentrations of T-AOC and T-SOD in both the liver and ovary. However, *Lp. plantarum* FRT4 intervention significantly increased the levels of T-AOC and T-SOD, and increased the mRNA expression level of antioxidant enzymes-related genes. The content of MDA was typically used as an index of lipid peroxidation and oxidative injury [46]. The increase of the concentrations of ALT and AST was regarded as the biomarker of issue damage [47, 48]. The contents of MDA, ALT, and AST in the liver and ovary of laying hens feeding HELP diet were significantly increased compared to the CT group, whereas the contents of MDA and ALT were significantly decreased after *Lp. plantarum* FRT4 intervention. These results indicate that *Lp. plantarum* FRT4 substantially alleviated hepatic and ovarian oxidative injury, and enhanced the antioxidant capacity in laying hens.

It is worth noting that OS could trigger inflammation and lead to the production of IL-1β and TNF-α [49]. TNF-α is a factor that stimulates and induces the production of reactive oxygen species (ROS) and lipid peroxidation, while also amplifying and prolonging inflammation [50]. Navasa et al. reported that TNF-α could induce the Kupffer cells to release IL-6 in the liver [51]. Moreover, the increase in TNF-α led to the accumulation of TG and steatosis, which in turn activated *NF-κB*, resulting in a vicious circle of worsening hepatic damage [52]. Generally, *IL-1β* is a pro-inflammatory factor, whereas *IL-10* has anti-inflammatory effects [53, 54]. In the FRT4M and FRT4H groups, the concentrations of IL-1β and

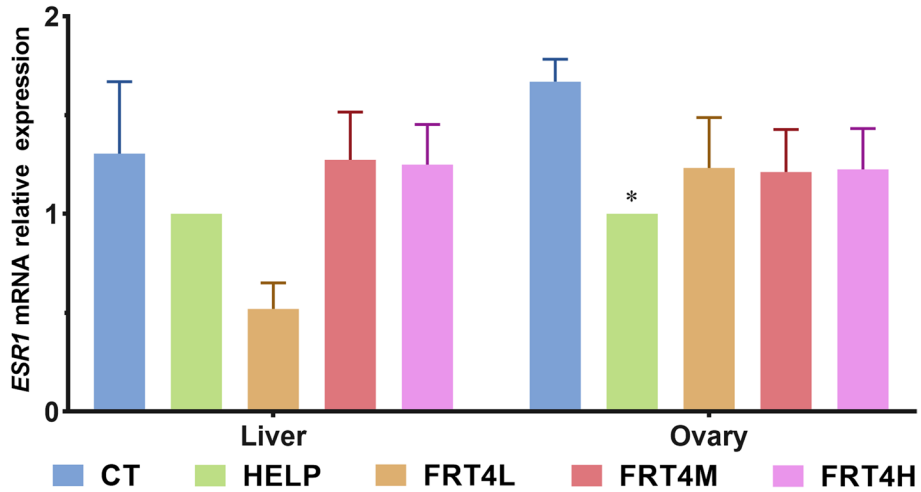


**Fig. 12** Effect of *Lp. plantarum* FRT4 on the mRNA expression level of *ESR1* in laying hens. The results were expressed as mean ± SEM, $n = 6$ hens per group. * indicates the significant difference between the HELP group and the CT group, and * indicates $P < 0.05$. CT: control group, hens fed with normal diet. HELP: model group, hens fed with high-energy low-protein diet. FRT4L, FRT4M, and FRT4H: experimental groups, hens fed with high-energy low-protein diet with $10^9$ CFU/kg, $10^{10}$ CFU/kg, and $10^{11}$ CFU/kg *Lp. plantarum* FRT4, respectively

TNF-α were significantly reduced in the liver and ovary compared to the HELP group. Additionally, the mRNA expression levels of *IL-1β* and *TNF*-α also decreased, and the mRNA expression level of *IL-10* was increased. MAFLD triggered excessive inflammatory reaction, and further activated the inflammation-related signaling pathways [55, 56]. *TLR-4*, expressed in hepatic stellate cells, activated *NF-κB* and the genes expression dependent on *NF-κB*, leading to an inflammatory response [57]. The mRNA expression levels of *TLR-4* and *NF-κB* of liver and ovary were upregulated in the HELP group compared to the CT group. Supplementation with *Lp. plantarum* FRT4 downregulated their expression levels. There results demonstrate that *Lp. plantarum* FRT4 improved inflammation by regulating the *TLR-4*/*NF-κB* pathway.

The occurrence of inflammation was closely to NLRP3 inflammasome, whose activity was crucial for maintaining cellular homeostasis and health [58]. The activation of the NLRP3 inflammasome has been observed in NAFLD [59], and is known to promote the development of inflammatory reactions [60]. Numerous researches suggested that inhibiting the *NLRP3* pathway could reduce hepatic inflammation and hepatocyte injury [61–64]. *Lp. plantarum* LP HJZW08 and its culture would prevent broilers from the inflammation infected with Salmonella by inhibiting *NLRP3* inflammasome and optimizing gut microbiota [65]. Feeding HELP diet caused the increase of the concentration and mRNA expression level of *NLRP*3 in the liver and ovary. After *Lp. plantarum* FRT4 intervention, the concentration and mRNA expression level of *NLRP*3 were decreased in the FR4M and FRT4H groups. Moreover, *NF-κB* can also activate the *NLRP3* inflammasome [66, 67]. These results indicated that *NLRP*3 may be another potential target through which *Lp. plantarum* FRT4 protect FLHS laying hen from serious inflammation reaction. However, it was found that different doses of *Lp. plantarum* FRT4 elicit distinct sensitivities in the antioxidant and anti-inflammatory responses in the liver and ovary. It has been established that hepatic metabolites can regulate ovarian function via the liver-blood-ovary axis in laying hens [68, 69]. Besides, gut microbiota and its associated metabolites play a crucial role in regulating liver function [70, 71]. Consequently, varying doses *Lp. plantarum* FRT4 exert differential regulatory effect on the gut microbiota and its metabolism, which in turn act on the liver and ovary by gut-liver axis and liver-blood-ovary axis. A previous study suggested that dietary intervention with varying doses could differently enhance antioxidation and anti-inflammation capabilities in the liver and ovary of laying hens [69]. Nevertheless, the specific regulatory mechanisms underlying the differential sensitivities of the liver and ovary to different doses of *Lp. plantarum* FRT4 still need further exploration.

Gut microbiota is the result of long-term co-evolution based on microorganism and hosts, which affects the physiological function of hosts and is influenced by the living environment and eating habits of the host [72]. Gut microbiota is the biggest metabolic sink in humans and animals [73]. According to metabolic results, 129 differential metabolites were identified in the FRT4M group compared to the HELP group, and these differential metabolites were enriched into 7 differential metabolic pathways, including tryptophan metabolism,

amino sugar and nucleotide sugar metabolism, galactose metabolism, insulin signaling pathway, FoxO signaling pathway, folate biosynthesis, and ubiquinone and other terpenoid-quinone biosynthesis. Tryptophan and its downstream metabolites have shown various health effects, including immune regulation, neurotransmitter regulation, and antioxidant activity [74–76]. Unabsorbed tryptophan is metabolized by the gut microbiota into indole and its derivatives, which play a beneficial role in the development of NAFLD and show the effect of improving liver steatosis and fibrosis [77]. Additionally, indole has physiological activity of stimulating the production of anti-inflammatory factors and inhibiting the generation of pro-inflammatory factors [78]. Xanthurenic acid has been proven to have strong antioxidant activity and physiological functions in protecting cells from DNA damage and lipid peroxidation [79]. According to reports, cholic acid and chenodeoxycholic acid were associated with inflammatory bowel disease and gastric mucosal intestinal metaplasia [80, 81]. In the present study, tryptophan metabolism was significantly upregulated in FRT4M group compared to the HELP group, with increased contents of metabolites related to tryptophan metabolism, such as indole, xanthurenic acid. Moreover, antioxidative enzymes activities were elevated and inflammatory factors were reduced in the liver and ovary. These results indicate that *Lp. plantarum* FRT4 could regulate tryptophan metabolism of gut microbiota to produce more bioactive substances to enhance the antioxidant capacity and reduce inflammation level in laying hens. FoxO family of transcription factors controls numerous biological functions in mammals [82], including the detoxification of oxidative stress [21, 83]. Both *FoxO1* and *FoxO3* had demonstrated potential activities in modulating lipid metabolism, exerting anti-inflammation effects, and enhancing antioxidant capacity. The activation of *AMPK-FoxO1* pathway and the interaction between sirtuin 1 (*SIRT1*) and *FoxO1* further regulate the expression of downstream gene *SOD*, thereby improving inflammation and OS associated with NAFLD and type 2 diabetes [84, 85]. FoxO3, a downstream target protein of *SIRT3*, enhances the transcription of FoxO-dependent *MnSOD* and *CAT*, and acts on the *ROS*/*Ras* signaling pathway, resulting in elimination of ROS and reduced OS injury [86]. The FoxO signaling pathway was significantly enriched in the FRT4M group compared to the HELP group, which was in accordance with the hepatic metabolic results in our previous study [39]. Furthermore, the qRT-PCR results showed that the mRNA expression levels of *FoxO1* and *FoxO3* were upregulated, as was the expression level of downstream gene *SOD*. These results are consistent with previous studies [87, 88]. Therefore, the FoxO signaling pathway is the important pathway for *Lp. plantarum* FRT4 relieving the OS induced by FLHS. Insulin signaling pathway is an important biochemical process, which affects the metabolism of lipids, glucose and proteins to a large extent. Abnormalities in insulin signaling pathway were related to several metabolic diseases such as diabetes and obesity [89]. Research has shown that under OS condition, the efficiency of insulin signaling decreases, leading to insulin resistance in cells [90]. The metabolism of amino sugars and nucleotide sugars plays an important role in the immune function decline caused by $H_2S$ resistance in laying hens [91]. In this study, the HELP diet significantly reduced antioxidant enzyme activity in the liver and ovary of laying hens, whereas these activities were increased in the FRT4M group. Meanwhile, the gut amino sugar and nucleotide sugar metabolism pathways and related metabolites in the FRT4M group were significantly upregulated compared to the HELP group, such as uridine diphosphate glucose acid, udp N-acetylglucosamine, and glucose, etc. These results indicate that the insulin signaling pathway and amino sugar and nucleotide sugar metabolism may represent additional potential regulatory target regulated by *Lp. plantarum* FRT4 to enhance the antioxidant and immunity capacities of laying hens.

Gut microbiota is the biggest and most complex microecosystem, and its composition and diversity play an irreplaceable role in nutrition metabolism, immunity, and adaptation to the environment in animals [92]. Numerous studies suggest that gut microbiota plays a key role in the development of NAFLD [93–95]. The gut dysbiosis was related to NAFLD, manifested as a decrease in beneficial flora and an increase in harmful flora [96]. The gut microbiota formation typically maintains a relatively stable state, and the dominant phyla were Bacteroidetes, Firmicutes, Proteobacteria and Actinobacteria [97–99]. The high abundance of Firmicutes and low abundance of Bacteroidetes are characteristics of NAFLD [100]. In this study, feeding HELP diet increased the abundance of Firmicutes in ceca and decreased the abundance of Bacteroidetes. In contrast, supplementation of *Lp. plantarum* FRT4 reduced the abundance of Firmicutes and increased the abundance of Bacteroidetes, which was more similar to the phylum level structural distribution of the CT group. Moreover, spearman correlation analysis showed that the abundances of Firmicutes and Bacteroidetes had a significant correlation with the antioxidant enzymes and the concentrations of inflammatory factors. Previous research has found that the abundance of Proteobacteria was reduced in the intestines of mice with NASH, while was increased after treatment with a methionine and choline-deficient diet [101]. Another study suggests that patients with NAFLD and NASH have higher abundance of Proteobacteria in their intestines [102]. After

feeding with HELP diet, the abundance of Proteobacteria in the intestine of laying hens was decreased, whereas the abundance was increased in the FRT4M group. These results indicate that Proteobacteria may play different regulatory roles in different contexts, and these differences may be related to species. *Prevotella* is a dominant genus of Bacteroidetes [103], is generally considered beneficial, contributing to polysaccharide degradation, SCFA metabolism, and glucose homeostasis [104, 105]. However, some studies indicated that *Prevotella* can be pathogenic and is related to multiple chronic inflammations [106, 107]. Whether *Prevotella* has a positive or negative effect may be related to the diversity at the strain-level diversity, which is influenced by interspecies and intraspecific variations [108]. Children typically had a higher abundance of *Prevotella* [109], while the adults had a lower abundance of *Prevotella* [110]. In this study, HELP diet reduced the abundance of *Prevotella* in ceca of laying hens compared to the CT group, whereas the FRT4M group had lower abundance of *Prevotella* compared to the HELP group. Further researches are needed to confirm the role of changes in *Prevotella* abundance in the progress of FLHS. *Alistipes* was another dominant genus. A study suggests that *Alistipes* is less abundant in intestines with severe liver fibrosis [111], which may promote the development of inflammation in NAFLD [112]. Chanda and De analyzed 3329 obese host-gut samples using a machine-learning-based approach, incorporating both 16S rRNA and metagenomic sequence data, which suggested a reduction in *Alistipes* species [113]. In this study, the HELP group exhibited a lower abundance of *Alistipes*, whereas the FRT4M group had a higher abundance. Furthermore, *Alistipes* was significantly positively correlated with T-SOD (antioxidative enzyme) and negatively correlated with MDA (lipid peroxidation marker). *Bacteroides* was significantly positively correlated with T-SOD and GSH-Px (antioxidative enzyme), and NLRP3 (inflammatory biomarker). These results suggest that *Alistipes* and *Bacteroides* played a key role in systemic antioxidant and anti-inflammation processes. A previous study had indicated that *Alistipes* and *Bacteroides* were often associated with SCFAs metabolism [114]. SCFAs, including acetate, butyrate, and propanoate, were reported to reduce systemic inflammation and OS [115, 116]. SCFAs were transported to organs and tissues via various SCFA transporter protein [117], thereby enhancing the host's antioxidant and anti-inflammation capabilities. Additionally, correlation analysis indicated that *Bacteroides* was significantly associated with *FoxO/TLR-4/NF-κB* signaling pathway in the liver. Thus, the genera *Alistipes* and *Bacteroides* may regulate gut SCFAs metabolism, thereby influencing the *FoxO/TLR-4/NF-κB* signaling pathway to alleviate hepatic and ovarian OS and inflammation.

Metagenomics can not only analyze the microbiota composition, but also the gene function of microbiota. Alanine, aspartate, and glutamate originate from intermediates in central metabolism, mainly from the citric acid cycle [118]. The basic product of the pentose phosphate pathway is pentose, which is used for nucleotide synthesis [119]. In this study, the HELP diet enhanced the gene function of pentose phosphate pathway in gut microbiota, coinciding with a significant increase in pro-inflammatory factors in the liver and ovary. A previous study showed that enhancing microbial function involved in the pentose phosphate pathway and arachidonic acid metabolism produced pro-inflammatory factors, which directly promoted host inflammatory damage [120]. In the FRT4M group, the gene function of pentose phosphate pathway in gut microbiota was reduced, which was consistent with the CT group. Additionally, the inflammation levels in the liver and ovary of the FRT4M group were greatly alleviated. These results indicate that *Lp. plantarum* FRT4 could alleviate inflammation reaction in laying hens by regulating the functional genes of pentose phosphate pathway in the gut microbiota. NOG3115 is annotated in the *AraC* family, a transcriptional regulatory factor. *AraC*-like transcription factors play a crucial role in regulating various physiological functions of bacteria, including carbon source metabolism, response to environmental stress, and pathogenesis [121]. Okeke et al. reported that the pathogenesis of enteroaggregative *Escherichia coli* (EAEC) involved colonization on the surface of the intestinal mucosa, mainly mediated by the production of enterotoxins and cytotoxics that disrupt host cells, inducing inflammation and diarrhea [122]. *AraC* was the main regulatory factor of EAEC virulence [123]. The function of NOG3115 was significantly enriched in the HELP group, but partially reversed in the FRT4M group. This suggests that *Lp. plantarum* FRT4 may regulate *AraC*-like transcription factors and alleviate intestinal barrier damage caused by the HELP diet in laying hens. Regarding carbohydrate enzyme gene function, significant differences were observed between groups in functional genes such as GT41, GT103, and PL6. GT41 mainly includes UDP GlcNAc: peptide beta N acetylglucosamine yltransfer (EC: 2.4.1.255); UDP Glc: peptide N-beta glucosyltransfer (EC: 2.4.1.-) and other related enzyme gene functions. Glucose enters the hexosamine pathway, producing UDP acetylglucosamine (UDP GlcNAc) as a donor for glycosylation [124]. *O*-GlcNAcylation was considered a nutrient and stress sensor and involved in transcription and translation, regulating signaling transduction and metabolic cellular processes

[125]. Previous studies have revealed the important role of hexosamine biosynthesis pathway and *O*-GlcNAcylation proteins in the development of diabetes, cancer and neurodegenerative diseases [126, 127]. The enrichment of GT41 functional genes was reduced in the HELP group but reversed in the FRT4M group, indicating that *Lp. plantarum* FRT4 could promote glucose metabolism in the gut microbiota of laying hens. PL6 primarily includes enzymes such as alginate lyase (EC: 4.2.2.3), chondroitinase B (EC: 4.2.2.19), MG specific initiate lyase (EC: 4.2.2. -), poly (alpha L guluronate) lyase/G specific initiate lyase (EC: 4.2.2.11) [128]. During the laying process, laying hens are often infected with *Salmonella*, causing intestinal inflammation and leading to a decrease in egg production rate [129]. Roque-Borda et al. investigated the anti-enteritis effect of alginate coated particles in a chicken model of *Salmonella* infection [130]. Their results showed that alginate coated particles significantly reduced *Salmonella* infection, particularly in terms of anti-inflammatory effects on the liver. In this study, the FRT4M group reversed the decrease in PL6 gene function caused by the HELP diet, indicating that *Lp. plantarum* FRT4 may have a physiological function of enhancing PL6 gene function in the gut microbiota of laying hens.

The production performance of laying hens is typically influenced by the levels of reproductive hormones. The estrogen level in laying hens at the later stage of laying is the direct reason for the sudden drop of laying rate, and is accompanied by a severe fatty liver incidence rate of 95% [131, 132]. Estrogen levels are associated with the progression of fatty liver, and a previous study has shown that endocrine hormones affect the development of fatty liver by interfering with lipid metabolism pathways [133]. $E_2$ is the main estrogen that maintains follicular development and maturation. The circulating level of $E_2$ was positively correlated with egg production rate and could promote the synthesis and transportation of triglycerides and cholesterol in the liver cells of laying hens [134]. Research suggests that increasing circulating estrogen levels was the key to alleviating ovarian degeneration and fatty liver in laying hens in the later stages of egg production [135], while a decrease in $E_2$ levels was the main reason for the decrease in egg production rate in the later stages of egg production [136]. In this study, the $E_2$ levels in the liver and ovary of the HELP group decreased, while the egg production rate also decreased [39]. However, after supplementation with *Lp. plantarum* FRT4, the $E_2$ levels in ovary of laying hens were significantly increased, and the egg production rate was also significantly increased [39]. FSH not only promotes the development of the fallopian tubes, ovaries, and stroma, but also plays a crucial role in follicular development and ovulation [137]. Previous research has shown that *Bacillus licheniformis* can increase serum FSH and $E_2$ levels in laying hens, thereby stimulating follicle growth and development [138]. Another study has shown that *Bacillus amyloliquefaciens* BLCC1-0238 could increase the levels of FSH and $E_2$, further increasing ovarian weight, promoting follicle growth and maturation [139], and thereby increasing egg laying rate in laying hens. In the present study, feeding HELP diet significantly reduced the content of FSH in the ovary of laying hens, while the contents of FSH in the FRT4L and FRT4H groups were significantly increased. According to the aforementioned theory, the significant increase in egg production rate in the *Lp. plantarum* FRT4 treatment groups is closely related to the increase of FSH and $E_2$ in the liver and ovary of laying hens. VTG is a precursor substance of yolk protein, produced in the liver and transported to eggs [140]. VTG was transported to and deposited in ovary to meet the nutritional requirements of the rapid development and maturation of the follicle [141]. The mRNA expression level of *VTG* was regulated by $E_2$ [142], resulting in low expression levels before egg-laying and high expression levels during egg-laying [143]. Therefore, VTG could serve as a biomarker for avian reproductive aging [144]. Additionally, $E_2$ acted on *ESR* to promote *VTG* mRNA expression [68, 69]. In the present study, the *ESR1* mRNA expression level was increased and the content of VTG in ovary was significantly increased after *Lp. plantarum* FRT4 intervention. The liver-blood-ovary axis has been reported to maintain the productional performance of aging hens by regulating functional substances such as $E_2$, VTG, FSH [68], and by improving the hepatic lipid metabolism [69]. However, FLHS induced by HELP diet caused OS and inflammation in the liver and ovary, leading to the functional disturbance of biosynthesis and transport. Consequently, the content of VTG was decreased in the liver and ovary of the HELP group. Supplementation with *Lp. plantarum* FRT4 significantly increased $E_2$, FSH, and VTG contents, as well as *ESR1* mRNA expression, thereby ameliorating the decline in reproductive performance resulting from lipid disturbance with FLHS. These results indicate that *Lp. plantarum* FRT4 can delay the reproductive aging of laying hens, prolong their egg laying cycle, and thus improve economic benefits.

## Conclusions

Collectively, the HELP diet induced OS and inflammation in the liver and ovary, as well as gut microbiota and its dysfuntion in laying hens. Supplementation with *Lp. plantarum* FRT4 enhanced antioxidant capacity, reduced inflammation level, and regulated the related-genes mRNA expression. *Lp. plantarum* FRT4 improved the gut microbiota composition and function, and modulated

the *FoxO*/*TLR-4*/*NF-κB* signaling pathway to prevent OS and inflammation of FLHS in laying hens. What's more, spearman analysis showed that the abundance of microbiota at different taxonomic levels was closely associated with antioxidant enzymes and inflammatory factors. Overall, *Lp. plantarum* FRT4 attenuated OS and inflammation of FLHS laying hens by regulating gut microbiota and its function, and further intervening in *FoxO*/*TLR-4*/*NF-κB* signaling pathway, thereby enhancing hepatic and ovarian function and increasing with estrogen levels. Meanwhile, there are some limits in this research that warrant attention and should be addressed in subsequent studies. Our findings indicate that different tissues respond differently to the effective doses of *Lp. plantarum* FRT4. Additionally, different doses of *Lp. plantarum* FRT4 had different antioxidation and anti-inflammation effects. These mechanisms of action should be addressed in future work.

**Abbreviations**

| | |
|---|---|
| ALT | Alanine aminotransferase |
| AST | Aspartate aminotransferase |
| CARD | Comprehensive antibiotic research database |
| CAT | Catalase |
| CAZy | Carbohydrate-active enzymes database |
| $E_2$ | Estradiol |
| FLHS | Fatty liver hemorrhage syndrome |
| FoxO | Forkhead box class O |
| FSH | Follicle-stimulating hormone |
| GSH-Px | Glutathione peroxidase |
| HELP | High-energy low-protein |
| IL-1β | Interleukin-1β |
| KEGG | Kyoto encyclopedia of genes and genomes |
| *Lp. plantarum* | *Lactiplantibacillus plantarum* |
| MAFLD | Metabolic-associated fatty liver disease |
| MDA | Malondialdehyde |
| MnSOD | Manganese superoxide dismutase |
| NAFLD | Non-alcoholic fatty liver disease |
| NF-κB | Nuclear factor kappa B |
| NLRP3 | NLR family pyrin domain containing 3 |
| OPLS-DA | Orthogonal partial least-squares-discriminant analysis |
| OS | Oxidative stress |
| ROS | Reactive oxygen species |
| SOD | Superoxide dismutase |
| T-AOC | Total-antioxidant capacity |
| TLRs | Toll-like receptors |
| TNF-α | Tumor necrosis factor α |
| VIP | Variable importance of projection |
| VTG | Vitellogenin |

## Supplementary Information

The online version contains supplementary material available at https://doi.org/10.1186/s40168-025-02083-0.

Additional file 1: Supplementary tables. Table S1 Compositions and nutrients contents of experimental diets. Table S2 The primer sequences for qRT-PCR. Table S3 Elution gradient. Table S4 Mass spectrometry parameters.

Additional file 2. Deposited data.

Additional file 3. Deposited data.

Additional file 4. Deposited data.

**Acknowledgements**
Not applicable.

**Authors' contributions**
DJL contributed to experimental design, performed experiments and collected samples, analyzed the data, wrote and revised the manuscript; KM, GHL, YSH, WWL, XX, and LYS interpreted the results; ZGW provided the funding; HYC contributed to experimental design, analyzed the data and revised the manuscript; PLY conceived the projected and provided the funding. All authors discussed the results and approved the final manuscript.

**Funding**
This research was supported by Science and Technology Innovation Project of the Chinese Academy of Agricultural Sciences (CAAS-ZDRW202303) and Science and Technology Innovation Project of IFR of Chinese Academy of Agricultural Sciences (CAAS-ASTIP-2023-IFR-13, IFR-ZDRW202301).

**Data availability**
The data analyzed during the current study are available from the corresponding author on reasonable request. The data that support the findings of this study have been deposited into CNGB Sequence Archive (CNSA) of China National GeneBank DataBase (CNGBdb) with accession number CNP0005501 (https://db.cngb.org/search/project/CNP0005501/ ).

## Declarations

**Ethics approval and consent to participate**
Generated statement: The animal study was reviewed and approved by The Institutional Animal Care and Use Committee of the Institute of Feed Research of Chinese Academy of Agricultural Sciences (IFR-CAAS20220729).

**Consent for publication**
Not applicable.

**Competing interests**
The authors declare no competing interests.

**Author details**
[1]Key Laboratory of Feed Biotechnology of Ministry of Agriculture and Rural Affairs, Institute of Feed Research, Chinese Academy of Agricultural Sciences, Beijing 100081, China.

Received: 6 May 2024 Accepted: 8 March 2025
Published online: 29 March 2025

**References**

1. Yamamura S, Eslam M, Kawaguchi T, Tsutsumi T, Nakano D, Yoshinaga S, et al. MAFLD identifies patients with significant hepatic fibrosis better than NAFLD. Liver Int. 2020;40(12):3018–30.
2. Chen W, Shi Y, Li G, Huang C, Zhuang Y, Shu B, et al. Preparation of the peroxisome proliferator-activated receptor α polyclonal antibody: Its application in fatty liver hemorrhagic syndrome. Int J Biol Macromol. 2021;182:179–86.
3. Chen Z, Tian R, She Z, Cai J, Li H. Role of oxidative stress in the pathogenesis of nonalcoholic fatty liver disease. Free Radic Biol Med. 2020;152:116–41.
4. Serviddio G, Bellanti F, Vendemiale G. Free radical biology for medicine: learning from nonalcoholic fatty liver disease. Free Radic Biol Med. 2013;65:952–68.
5. Luo Z, Chen Z, Hu J, Ding G. Interplay of lipid metabolism and inflammation in podocyte injury. Metabolism. 2024;150:155718.
6. Wang J, Jia R, Gong H, Celi P, Zhuo Y, Ding X, et al. The effect of oxidative stress on the chicken ovary: involvement of microbiota and melatonin interventions. Antioxidants (Basel). 2021;10(9):1422.
7. Lassmann H, van Horssen J, Mahad D. Progressive multiple sclerosis: pathology and pathogenesis. Nat Rev Neurol. 2012;8(11):647–56.

8. Yuan T, Yang T, Chen H, Fu D, Hu Y, Wang J, et al. New insights into oxidative stress and inflammation during diabetes mellitus-accelerated atherosclerosis. Redox Biol. 2019;20:247–60.
9. Liu D, Gao X, Pan XF, Zhou T, Zhu C, Li F, et al. The hepato-ovarian axis: genetic evidence for a causal association between non-alcoholic fatty liver disease and polycystic ovary syndrome. BMC Med. 2023;21(1):62.
10. Wu H, Liu Q, Yang N, Xu S. Polystyrene-microplastics and DEHP co-exposure induced DNA damage, cell cycle arrest and necroptosis of ovarian granulosa cells in mice by promoting ROS production. Sci Total Environ. 2023;871:161962.
11. Maldonado SS, Cedars MI, Yates KP, Wilson LA, Gill R, Terrault NA, et al. Antimullerian hormone, a marker of ovarian reserve, is protective against presence and severity of NASH in premenopausal women. Clin Gastroenterol Hepatol. 2024;22(2):339–46.
12. Cogger VC, Muller M, Fraser R, McLean AJ, Khan J, Le Couteur DG. The effects of oxidative stress on the liver sieve. J Hepatol. 2004;41(3):370–6.
13. Yan F, Zhao Q, Li Y, Zheng Z, Kong X, Shu C, et al. The role of oxidative stress in ovarian aging: a review. J Ovarian Res. 2022;15(1):100.
14. Wang X, Yang J, Li H, Mu H, Zeng L, Cai S, et al. MiR-484 mediates oxidative stress-induced ovarian dysfunction and promotes granulosa cell apoptosis via SESN2 downregulation. Redox Biol. 2023;62:102684.
15. Bao T, Yao J, Zhou S, Ma Y, Dong J, Zhang C, et al. Naringin prevents follicular atresia by inhibiting oxidative stress in the aging chicken. Poult Sci. 2022;101(7):101891.
16. Liu Q, Li W, Huang S, Zhao L, Zhang J, Ji C, et al. R- Is superior to S-form of α-lipoic acid in anti-inflammatory and antioxidant effects in laying Hens. Antioxidants (Basel). 2022;11(8):1530.
17. Rodriguez-Colman MJ, Dansen TB, Burgering BMT. FOXO transcription factors as mediators of stress adaptation. Nat Rev Mol Cell Biol. 2024;25(1):46–64.
18. Tang S, Cheng Y, Xu T, Wu T, Pan S, Xu X. Hypoglycemic effect of *Lactobacillus plantarum*-fermented mulberry pomace extract *in vitro* and in *Caenorhabditis elegans*. Food Funct. 2023;14(20):9253–64.
19. Lee SS, Kennedy S, Tolonen AC, Ruvkun G. DAF-16 target genes that control C. elegans life-span and metabolism. Science. 2003;300(5619):644–7.
20. Klotz LO, Sánchez-Ramos C, Prieto-Arroyo I, Urbánek P, Steinbrenner H, Monsalve M. Redox regulation of FoxO transcription factors. Redox Biol. 2015;6:51–72.
21. Kops GJ, Dansen TB, Polderman PE, Saarloos I, Wirtz KW, Coffer PJ, et al. Forkhead transcription factor FOXO3a protects quiescent cells from oxidative stress. Nature. 2002;419(6904):316–21.
22. Song J, Li Z, Zhou L, Chen X, Sew WQG, Herranz H, et al. FOXO-regulated OSER1 reduces oxidative stress and extends lifespan in multiple species. Nat Commun. 2024;15(1):7144.
23. Lee JW, Nam H, Kim LE, Jeon Y, Min H, Ha S, et al. TLR4 (toll-like receptor 4) activation suppresses autophagy through inhibition of FOXO3 and impairs phagocytic capacity of microglia. Autophagy. 2019;15(5):753–70.
24. Guo Q, Jin Y, Chen X, Ye X, Shen X, Lin M, et al. NF-κB in biology and targeted therapy: new insights and translational implications. Signal Transduct Target Ther. 2024;9(1):53.
25. Capece D, D'Andrea D, Begalli F, Goracci L, Tornatore L, Alexander JL, et al. Enhanced triacylglycerol catabolism by carboxylesterase 1 promotes aggressive colorectal carcinoma. J Clin Invest. 2021;131(11):e137845.
26. Tao Y, Xu L, Liu X, Wang P, Wei S, Huang Y, et al. Chitosan-coated artesunate protects against ulcerative colitis via STAT6-mediated macrophage M2 polarization and intestinal barrier protection. Int J Biol Macromol. 2024;254(Pt 1):127680.
27. Pal S, Sahu A, Verma R, Haldar C. BPS-induced ovarian dysfunction: Protective actions of melatonin via modulation of SIRT-1/Nrf2/NFκB and IR/PI3K/pAkt/GLUT-4 expressions in adult golden hamster. J Pineal Res. 2023;75(1):e12869.
28. Feng T, Wang J. Oxidative stress tolerance and antioxidant capacity of lactic acid bacteria as probiotic: a systematic review. Gut Microbes. 2020;12(1):1801944.
29. Jänsch A, Freiding S, Behr J, Vogel RF. Contribution of the NADH-oxidase (Nox) to the aerobic life of *Lactobacillus sanfranciscensis* DSM20451T. Food Microbiol. 2011;28(1):29–37.
30. Kono Y, Fridovich I. Isolation and characterization of the pseudocatalase of *Lactobacillus plantarum*. J Biol Chem. 1983;258(10):6015–9.
31. Liu L, Deng L, Wei W, Li C, Lu Y, Bai J, et al. *Lactiplantibacillus plantarum* LPJZ-658 Improves Non-Alcoholic Steatohepatitis by Modulating Bile Acid Metabolism and Gut Microbiota in Mice. Int J Mol Sci. 2023;24(18):13997.
32. Kim DY, Park JY, Gee HY. *Lactobacillus plantarum* ameliorates NASH-related inflammation by upregulating L-arginine production. Exp Mol Med. 2023;55(11):2332–45.
33. Teng Q, Lv H, Peng L, Ren Z, Chen J, Ma L, et al. *Lactiplantibacillus plantarum* ZDY2013 inhibits the development of non-alcoholic fatty liver disease by regulating the intestinal microbiota and modulating the PI3K/Akt pathway. Nutrients. 2024;16(7):958.
34. Yuan J, Zhao F, Liu Y, Liu H, Zhang K, Tian X, et al. Effects of *Lactiplantibacillus plantarum* on oxidative stress, mitophagy, and NLRP3 inflammasome activation in broiler breast meat. Poult Sci. 2023;102(12):103128.
35. Zhao J, Zhao F, Li X, Yuan J, Zhang K, Liu H, et al. Multi-omics reveals the mechanisms underlying *Lactiplantibacillus plantarum* P8-mediated attenuation of oxidative stress in broilers challenged with dexamethasone. Anim Nutr. 2023;14:281–302.
36. Yuan J, Liu Y, Zhao F, Mu Y, Tian X, Liu H, et al. Hepatic proteomics analysis reveals attenuated endoplasmic reticulum stress in *Lactiplantibacillus plantarum*-treated oxidatively stressed broilers. J Agric Food Chem. 2023;71(30):11726–39.
37. Jian H, Li R, Huang X, Li J, Li Y, Ma J, et al. Branched-chain amino acids alleviate NAFLD via inhibiting de novo lipogenesis and activating fatty acid β-oxidation in laying hens. Redox Biol. 2024;77:103385.
38. Miao S, Mu T, Li R, Li Y, Zhao W, Li J, et al. Coated sodium butyrate ameliorates high-energy and low-protein diet induced hepatic dysfunction via modulating mitochondrial dynamics, autophagy and apoptosis in laying hens. J Anim Sci Biotechnol. 2024;15(1):15.
39. Li D, Cai H, Liu G, Han Y, Qiu K, Liu W, et al. *Lactiplantibacillus plantarum* FRT4 attenuates high-energy low-protein diet-induced fatty liver hemorrhage syndrome in laying hens through regulating gut-liver axis. J Anim Sci Biotechnol. 2024;15(1):31.
40. Dale N. National research council nutrient requirements of poultry-ninth revised edition (1994). J Appl Poultry Res. 1994;3(1):101.
41. Rutkowski JM, Davis KE, Scherer PE. Mechanisms of obesity and related pathologies: the macro- and microcirculation of adipose tissue. FEBS J. 2009;276(20):5738–46.
42. Yuan Y, He J, Tang M, Chen H, Wei T, Zhang B, et al. Preventive effect of Ya'an Tibetan tea on obesity in rats fed with a hypercaloric high-fat diet revealed by gut microbiology and metabolomics studies. Food Res Int. 2023;165:112520.
43. Gunasekar SK, Heebink J, Carpenter DH, Kumar A, Xie L, Zhang H, et al. Adipose-targeted SWELL1 deletion exacerbates obesity- and age-related nonalcoholic fatty liver disease. JCI Insight. 2023;8(5):e154940.
44. Ye Q, Liu Y, Zhang G, Deng H, Wang X, Tuo L, et al. Deficiency of gluconeogenic enzyme PCK1 promotes metabolic-associated fatty liver disease through PI3K/AKT/PDGF axis activation in male mice. Nat Commun. 2023;14(1):1402.
45. Yang X, Li D, Zhang M, Feng Y, Jin X, Liu D, et al. Ginkgo biloba extract alleviates fatty liver hemorrhagic syndrome in laying hens via reshaping gut microbiota. J Anim Sci Biotechnol. 2023;14(1):97.
46. Zhou YH, Yu JP, Liu YF, Teng XJ, Ming M, Lv P, et al. Effects of Ginkgo biloba extract on inflammatory mediators (SOD, MDA, TNF-alpha, NF-kappaBp65, IL-6) in TNBS-induced colitis in rats. Mediators Inflamm. 2006;2006(5):92642.
47. Fox T, Gould S, Princy N, Rowland T, Lutje V, Kuehn R. Therapeutics for treating mpox in humans. Cochrane Database Syst Rev. 2023;3(3):CD015769.
48. Wang Z, Zang L, Ren W, Guo H, Sheng N, Zhou X, et al. Bile acid metabolism disorder mediates hepatotoxicity of Nafion by-product 2 and perfluorooctane sulfonate in male PPARα-KO mice. Sci Total Environ. 2023;876:162579.
49. Wu J, Sun X, Wu C, Hong X, Xie L, Shi Z, et al. Single-cell transcriptome analysis reveals liver injury induced by glyphosate in mice. Cell Mol Biol Lett. 2023;28(1):11.
50. Larrick JW, Wright SC. Cytotoxic mechanism of tumor necrosis factor-alpha. FASEB J. 1990;4(14):3215–23.

51. Navasa M, Gordon DA, Hariharan N, Jamil H, Shigenaga JK, Moser A, et al. Regulation of microsomal triglyceride transfer protein mRNA expression by endotoxin and cytokines. J Lipid Res. 1998;39(6):1220–30.
52. Feldstein AE, Werneburg NW, Canbay A, Guicciardi ME, Bronk SF, Rydzewski R, et al. Free fatty acids promote hepatic lipotoxicity by stimulating TNF-alpha expression via a lysosomal pathway. Hepatology. 2004;40(1):185–94.
53. Senn JJ, Klover PJ, Nowak IA, Mooney RA. Interleukin-6 induces cellular insulin resistance in hepatocytes. Diabetes. 2002;51(12):3391–9.
54. Malavige GN, Gomes L, Alles L, Chang T, Salimi M, Fernando S, et al. Serum IL-10 as a marker of severe dengue infection. BMC Infect Dis. 2013;13:341.
55. Ma Y, Gao M, Liu D. Chlorogenic acid improves high fat diet-induced hepatic steatosis and insulin resistance in mice. Pharm Res. 2015;32(4):1200–9.
56. Xu M, Ge C, Qin Y, Gu T, Lv J, Wang S, et al. Activated TNF-α/RIPK3 signaling is involved in prolonged high fat diet-stimulated hepatic inflammation and lipid accumulation: inhibition by dietary fisetin intervention. Food Funct. 2019;10(3):1302–16.
57. Bessone F, Razori MV, Roma MG. Molecular pathways of nonalcoholic fatty liver disease development and progression. Cell Mol Life Sci. 2019;76(1):99–128.
58. Sharma BR, Kanneganti TD. NLRP3 inflammasome in cancer and metabolic diseases. Nat Immunol. 2021;22(5):550–9.
59. Mridha AR, Wree A, Robertson AAB, Yeh MM, Johnson CD, Van Rooyen DM, et al. NLRP3 inflammasome blockade reduces liver inflammation and fibrosis in experimental NASH in mice. J Hepatol. 2017;66(5):1037–46.
60. Nie B, Liu X, Lei C, Liang X, Zhang D, Zhang J. The role of lysosomes in airborne particulate matter-induced pulmonary toxicity. Sci Total Environ. 2024;919:170893.
61. Csak T, Pillai A, Ganz M, Lippai D, Petrasek J, Park JK, et al. Both bone marrow-derived and non-bone marrow-derived cells contribute to AIM2 and NLRP3 inflammasome activation in a MyD88-dependent manner in dietary steatohepatitis. Liver Int. 2014;34(9):1402–13.
62. Szabo G, Petrasek J. Inflammasome activation and function in liver disease. Nat Rev Gastroenterol Hepatol. 2015;12(7):387–400.
63. Wree A, Eguchi A, McGeough MD, Pena CA, Johnson CD, Canbay A, et al. NLRP3 inflammasome activation results in hepatocyte pyroptosis, liver inflammation, and fibrosis in mice. Hepatology. 2014;59(3):898–910.
64. He S, Li Z, Wang L, Yao N, Wen H, Yuan H, et al. A nanoenzyme-modified hydrogel targets macrophage reprogramming-angiogenesis crosstalk to boost diabetic wound repair. Bioact Mater. 2024;35:17–30.
65. Guan L, Hu A, Ma S, Liu J, Yao X, Ye T, et al. *Lactiplantibacillus plantarum* postbiotic protects against *Salmonella* infection in broilers via modulating NLRP3 inflammasome and gut microbiota. Poult Sci. 2024;103(4):103483.
66. Haneklaus M, O'Neill LA, Coll RC. Modulatory mechanisms controlling the NLRP3 inflammasome in inflammation: recent developments. Curr Opin Immunol. 2013;25(1):40–5.
67. Schroder K, Zhou R, Tschopp J. The NLRP3 inflammasome: a sensor for metabolic danger? Science. 2010;327(5963):296–300.
68. Wu L, Lv Y, Ge C, Luo X, Hu Z, Huang W, et al. Polysaccharide from *Hericium erinaceus* improved laying performance of aged hens by promoting yolk precursor synthesis and follicle development via liver-blood-ovary axis. Poult Sci. 2024;103(7):103810.
69. Wu H, Yuan J, Yin H, Jing B, Sun C, Nguepi Tsopmejio IS, et al. *Flammulina velutipes* stem regulates oxidative damage and synthesis of yolk precursors in aging laying hens by regulating the liver-blood-ovary axis. Poult Sci. 2023;102(1):102261.
70. Raya Tonetti F, Eguileor A, Mrdjen M, Pathak V, Travers J, Nagy LE, et al. Gut-liver axis: Recent concepts in pathophysiology in alcohol-associated liver disease. Hepatology. 2024;80(6):1342–71.
71. Ghosh S, Zhao X, Alim M, Brudno M, Bhat M. Artificial intelligence applied to 'omics data in liver disease: towards a personalised approach for diagnosis, prognosis and treatment. Gut. 2025;74(2):295–311.
72. Spor A, Koren O, Ley R. Unravelling the effects of the environment and host genotype on the gut microbiome. Nat Rev Microbiol. 2011;9(4):279–90.
73. Chen J, Vitetta L. Gut microbiota metabolites in NAFLD pathogenesis and therapeutic implications. Int J Mol Sci. 2020;21(15):5214.
74. Fiore A, Murray PJ. Tryptophan and indole metabolism in immune regulation. Curr Opin Immunol. 2021;70:7–14.
75. Davidson M, Rashidi N, Nurgali K, Apostolopoulos V. The Role of tryptophan metabolites in neuropsychiatric disorders. Int J Mol Sci. 2022;23(17):9968.
76. Xu K, Liu G, Fu C. The tryptophan pathway targeting antioxidant capacity in the placenta. Oxid Med Cell Longev. 2018;2018:1054797.
77. Dai X, Hou H, Zhang W, Liu T, Li Y, Wang S, et al. Microbial metabolites: critical regulators in NAFLD. Front Microbiol. 2020;11:567654.
78. Sun J, Zhang Y, Kong Y, Ye T, Yu Q, Kumaran Satyanarayanan S, et al. Microbiota-derived metabolite Indoles induced aryl hydrocarbon receptor activation and inhibited neuroinflammation in APP/PS1 mice. Brain Behav Immun. 2022;106:76–88.
79. Murakami K, Ito M, Yoshino M. Xanthurenic acid inhibits metal ion-induced lipid peroxidation and protects NADP-isocitrate dehydrogenase from oxidative inactivation. J Nutr Sci Vitaminol (Tokyo). 2001;47(4):306–10.
80. Chen L, Jiao T, Liu W, Luo Y, Wang J, Guo X, et al. Hepatic cytochrome P450 8B1 and cholic acid potentiate intestinal epithelial injury in colitis by suppressing intestinal stem cell renewal. Cell Stem Cell. 2022;29(9):1366–81.
81. Lu W, Ni Z, Jiang S, Tong M, Zhang J, Zhao J, et al. Resveratrol inhibits bile acid-induced gastric intestinal metaplasia via the PI3K/AKT/p-FoxO4 signalling pathway. Phytother Res. 2021;35(3):1495–507.
82. Brunet A, Sweeney LB, Sturgill JF, Chua KF, Greer PL, Lin Y, et al. Stress-dependent regulation of FOXO transcription factors by the SIRT1 deacetylase. Science. 2004;303(5666):2011–5.
83. Nemoto S, Finkel T. Redox regulation of forkhead proteins through a p66shc-dependent signaling pathway. Science. 2002;295(5564):2450–2.
84. Nam H, Lim JH, Kim TW, Kim EN, Oum SJ, Bae SH, et al. Extracellular superoxide dismutase attenuates hepatic oxidative stress in nonalcoholic fatty liver disease through the adenosine monophosphate-activated protein kinase activation. Antioxidants (Basel). 2023;12(12):2040.
85. Chen H, Guo J, Cai Y, Zhang C, Wei F, Sun H, et al. Elucidation of the anti-β-cell dedifferentiation mechanism of a modified Da Chaihu Decoction by an integrative approach of network pharmacology and experimental verification. J Ethnopharmacol. 2024;321:117481.
86. Jin W, Li C, Yang S, Song S, Hou W, Song Y, et al. Hypolipidemic effect and molecular mechanism of ginsenosides: a review based on oxidative stress. Front Pharmacol. 2023;14:1166898.
87. Krishnan UA, Viswanathan P, Venkataraman AC. AMPK activation by AICAR reduces diet induced fatty liver in C57BL/6 mice. Tissue Cell. 2023;82:102054.
88. Teranishi M, Ito M, Huang Z, Nishiyama Y, Masuda A, Mino H, et al. Extremely low-frequency electromagnetic field (ELF-EMF) increases mitochondrial electron transport chain activities and ameliorates depressive behaviors in mice. Int J Mol Sci. 2024;25(20):11315.
89. Feng W, Xu Y, Su S, Yu F, Li J, Jia R, et al. Transcriptomic analysis of hydrogen peroxide-induced liver dysfunction in *Cyprinus carpio*: Insights into protein synthesis and metabolism. Sci Total Environ. 2024;917:170393.
90. Eriksson JW. Metabolic stress in insulin's target cells leads to ROS accumulation - a hypothetical common pathway causing insulin resistance. FEBS Lett. 2007;581(19):3734–42.
91. Wu G, Zhou T, Ma P, Xie B, Li W, Gong S, et al. Mechanism determination on the interactive effects between host immunity and gut microbiome to resist consecutive hydrogen sulfide inhalation of laying hens. Poult Sci. 2023;102(7):102694.
92. Zhang Z, Bao C, Li Z, He C, Jin W, Li C, et al. Integrated omics analysis reveals the alteration of gut microbiota and fecal metabolites in *Cervus elaphus kansuensis*. Appl Microbiol Biotechnol. 2024;108(1):125.
93. Wu Y, Yin W, Hao P, Chen Y, Yu L, Yu X, et al. Polysaccharide from *Panax japonicus* C.A. Mey prevents non-alcoholic fatty liver disease development based on regulating liver metabolism and gut microbiota in mice. Int J Biol Macromol. 2024;260(Pt 1):129430.

94. Ding Y, Yanagi K, Yang F, Callaway E, Cheng C, Hensel ME, et al. Oral supplementation of gut microbial metabolite indole-3-acetate alleviates diet-induced steatosis and inflammation in mice. Elife. 2024;12:RP87458.
95. Bilson J, Oquendo CJ, Read J, Scorletti E, Afolabi PR, Lord J, et al. Markers of adipose tissue fibrogenesis associate with clinically significant liver fibrosis and are unchanged by synbiotic treatment in patients with NAFLD. Metabolism. 2024;151:155759.
96. Su X, Chen S, Liu J, Feng Y, Han E, Hao X, et al. Composition of gut microbiota and non-alcoholic fatty liver disease: A systematic review and meta-analysis. Obes Rev. 2024;25(1):e13646.
97. Ponsuksili S, Hadlich F, Perdomo-Sabogal A, Reyer H, Oster M, Trakooljul N, et al. The dynamics of molecular, immune and physiological features of the host and the gut microbiome, and their interactions before and after onset of laying in two hen strains. Poult Sci. 2023;102(1):102256.
98. Feng J, Li Z, Ma H, Yue Y, Hao K, Li J, et al. Quercetin alleviates intestinal inflammation and improves intestinal functions via modulating gut microbiota composition in LPS-challenged laying hens. Poult Sci. 2023;102(3):102433.
99. Zhou J, Fu Y, Qi G, Dai J, Zhang H, Wang J, et al. Yeast cell-wall polysaccharides improve immunity and attenuate inflammatory response via modulating gut microbiota in LPS-challenged laying hens. Int J Biol Macromol. 2023;224:407–21.
100. Loomba R, Seguritan V, Li W, Long T, Klitgord N, Bhatt A, et al. Gut microbiome-based metagenomic signature for non-invasive detection of advanced fibrosis in human nonalcoholic fatty liver disease. Cell Metab. 2019;30(3):607.
101. Su C, Wang J, Luo H, Chen J, Lin F, Mo J, et al. Gut microbiota plays essential roles in soyasaponin's preventive bioactivities against steatohepatitis in the methionine and choline deficient (MCD) diet-induced non-alcoholic steatohepatitis (NASH) mice. Mol Nutr Food Res. 2024;68(4):e2300561.
102. Abdollahiyan S, Nabavi-Rad A, Keshavarz Azizi Raftar S, Monnoye M, Salarieh N, Farahanie A, et al. Characterization of gut microbiome composition in Iranian patients with nonalcoholic fatty liver disease and nonalcoholic steatohepatitis. Sci Rep. 2023;13(1):20584.
103. Ley RE. Gut microbiota in 2015: Prevotella in the gut: choose carefully. Nat Rev Gastroenterol Hepatol. 2016;13(2):69–70.
104. Kovatcheva-Datchary P, Nilsson A, Akrami R, Lee YS, De Vadder F, Arora T, et al. Dietary fiber-induced improvement in glucose metabolism is associated with increased abundance of *Prevotella*. Cell Metab. 2015;22(6):971–82.
105. De Filippis F, Pellegrini N, Vannini L, Jeffery IB, La Storia A, Laghi L, Serrazanetti DI, et al. High-level adherence to a Mediterranean diet beneficially impacts the gut microbiota and associated metabolome. Gut. 2016;65(11):1812–21.
106. Tett A, Pasolli E, Masetti G, Ercolini D, Segata N. Prevotella diversity, niches and interactions with the human host. Nat Rev Microbiol. 2021;19(9):585–99.
107. Larsen JM. The immune response to Prevotella bacteria in chronic inflammatory disease. Immunology. 2017;151(4):363–74.
108. Long Q, Luo F, Li B, Li Z, Guo Z, Chen Z, et al. Gut microbiota and metabolic biomarkers in metabolic dysfunction-associated steatotic liver disease. Hepatol Commun. 2024;8(3):e0310.
109. Michail S, Lin M, Frey MR, Fanter R, Paliy O, Hilbush B, et al. Altered gut microbial energy and metabolism in children with non-alcoholic fatty liver disease. FEMS Microbiol Ecol. 2015;91(2):1–9.
110. Shen F, Zheng RD, Sun XQ, Ding WJ, Wang XY, Fan JG. Gut microbiota dysbiosis in patients with non-alcoholic fatty liver disease. Hepatobiliary Pancreat Dis Int. 2017;16(4):375–81.
111. Schwenger KJP, Sharma D, Ghorbani Y, Xu W, Lou W, Comelli EM, et al. Links between gut microbiome, metabolome, clinical variables and non-alcoholic fatty liver disease severity in bariatric patients. Liver Int. 2024;44(5):1176–88.
112. Lee G, You HJ, Bajaj JS, Joo SK, Yu J, Park S, et al. Distinct signatures of gut microbiome and metabolites associated with significant fibrosis in non-obese NAFLD. Nat Commun. 2020;11(1):4982.
113. Chanda D, De D. Meta-analysis reveals obesity associated gut microbial alteration patterns and reproducible contributors of functional shift. Gut Microbes. 2024;16(1):2304900.
114. Bacil GP, Romualdo GR, Rodrigues J, Barbisan LF. Indole-3-carbinol and chlorogenic acid combination modulates gut microbiome and attenuates nonalcoholic steatohepatitis in a murine model. Food Res Int. 2023;174(Pt 1):113513.
115. Canfora EE, Jocken JW, Blaak EE. Short-chain fatty acids in control of body weight and insulin sensitivity. Nat Rev Endocrinol. 2015;11(10):577–91.
116. Rekha K, Venkidasamy B, Samynathan R, Nagella P, Rebezov M, Khayrullin M, et al. Short-chain fatty acid: An updated review on signaling, metabolism, and therapeutic effects. Crit Rev Food Sci Nutr. 2024;64(9):2461–89.
117. Martin-Gallausiaux C, Marinelli L, Blottière HM, Larraufie P, Lapaque N. SCFA: mechanisms and functional importance in the gut. Proc Nutr Soc. 2021;80(1):37–49.
118. Zheng H, Jiang J, Huang C, Wang X, Hu P. Effect of sugar content on characteristic flavour formation of tomato sour soup fermented by *Lacticaseibacillus casei* H1 based on non-targeted metabolomics analysis. Food Chem X. 2024;21:101116.
119. Chatzinikolaou PN, Margaritelis NV, Paschalis V, Theodorou AA, Vrabas IS, Kyparos A, et al. Erythrocyte metabolism. Acta Physiol (Oxf). 2024;240(3):e14081.
120. Chen Q, Luo Y, Shen Y, Li X, Yang H, Li J, et al. Fructose corn syrup induces inflammatory injury and obesity by altering gut microbiota and gut microbiota-related arachidonic acid metabolism. J Nutr Biochem. 2024;124: 109527.
121. Pearson AN, Incha MR, Ho CN, Schmidt M, Roberts JB, Nava AA, et al. Characterization and diversification of AraC/XylS family regulators guided by transposon sequencing. ACS Synth Biol. 2024;13(1):206–19.
122. Okeke IN, Nataro JP. Enteroaggregative *Escherichia coli*. Lancet Infect Dis. 2001;1(5):304–13.
123. Rodriguez-Valverde D, Giron JA, Hu Y, Nataro JP, Ruiz-Perez F, Santiago AE. Highly-conserved regulatory activity of the ANR family in the virulence of diarrheagenic bacteria through interaction with master and global regulators. Sci Rep. 2023;13(1):7024.
124. Yang X, Qian K. Protein O-GlcNAcylation: emerging mechanisms and functions. Nat Rev Mol Cell Biol. 2017;18(7):452–65.
125. Hardivillé S, Hart GW. Nutrient regulation of signaling, transcription, and cell physiology by O-GlcNAcylation. Cell Metab. 2014;20(2):208–13.
126. Lu S, Liao Z, Lu X, Katschinski DM, Mercola M, Chen J, et al. Hyperglycemia acutely increases cytosolic reactive oxygen species via *O*-linked GlcNAcylation and CaMKII activation in mouse ventricular myocytes. Circ Res. 2020;126(10):e80–96.
127. Covert JD, Grice BA, Thornburg MG, Kaur M, Ryan AP, Tackett L, et al. An early, reversible cholesterolgenic etiology of diet-induced insulin resistance. Mol Metab. 2023;72:101715.
128. Gu X, Fu L, Wang Z, Cao Z, Zhao L, Seswita-Zilda D, et al. A novel bifunctional alginate lyase and antioxidant activity of the enzymatic hydrolysates. J Agric Food Chem. 2024;72(8):4116–26.
129. Jan TR, Lin CS, Yang WY. Differential cytokine profiling and microbial species involved in cecal microbiota modulations in SPF chicks immunized with a dual vaccine against *Salmonella Typhimurium* infection. Poult Sci. 2024;103(2):103334.
130. Roque-Borda CA, Souza Saraiva MM, Monte DFM, Rodrigues Alves LB, de Almeida AM, Ferreira TS, et al. HPMCAS-coated alginate microparticles loaded with Ctx(Ile$^{21}$)-Ha as a promising antimicrobial agent against *Salmonella Enteritidis* in a chicken infection model. ACS Infect Dis. 2022;8(3):472–81.
131. Della TS. Non-alcoholic fatty liver disease as a canonical example of metabolic inflammatory-based liver disease showing a sex-specific prevalence: relevance of estrogen signaling. Front Endocrinol (Lausanne). 2020;11:572490.
132. Lonardo A, Nascimbeni F, Ballestri S, Fairweather D, Win S, Than TA, et al. Sex differences in nonalcoholic fatty liver disease: state of the art and identification of research gaps. Hepatology. 2019;70(4):1457–69.
133. Kur P, Kolasa-Wołosiuk A, Misiakiewicz-Has K, Wiszniewska B. Sex hormone-dependent physiology and diseases of liver. Int J Environ Res Public Health. 2020;17(8):2620.
134. Zhang DD, Wang DD, Wang Z, Wang YB, Li GX, Sun GR, et al. Estrogen abolishes the repression role of gga-miR-221-5p targeting *ELOVL6* and *SQLE* to promote lipid synthesis in chicken liver. Int J Mol Sci. 2020;21(5):1624.

135. Yao H, Hu Y, Tong H, Shi S. Dimethylglycine alleviates metabolic dysfunction-associated fatty liver disease by improving the circulating estrogen level via gut *Staphylococcus*. J Agric Food Chem. 2024;72(5):2708–17.
136. Wu H, Li H, Hou Y, Huang L, Hu J, Lu Y, et al. Differences in egg yolk precursor formation of Guangxi Ma chickens with dissimilar laying rate at the same or various ages. Theriogenology. 2022;184:13–25.
137. Lu Z, Zeng N, Jiang S, Wang X, Yan H, Gao C. Dietary replacement of soybean meal by fermented feedstuffs for aged laying hens: effects on laying performance, egg quality, nutrient digestibility, intestinal health, follicle development, and biological parameters in a long-term feeding period. Poult Sci. 2023;102(3):102478.
138. Lei K, Li YL, Yu DY, Rajput IR, Li WF. Influence of dietary inclusion of *Bacillus licheniformis* on laying performance, egg quality, antioxidant enzyme activities, and intestinal barrier function of laying hens. Poult Sci. 2013;92(9):2389–95.
139. Zhou Y, Li S, Pang Q, Miao Z. *Bacillus amyloliquefaciens* BLCC1-0238 can effectively improve laying performance and egg quality via enhancing immunity and regulating reproductive hormones of laying hens. Probiotics Antimicrob Proteins. 2020;12(1):246–52.
140. Brawand D, Wahli W, Kaessmann H. Loss of egg yolk genes in mammals and the origin of lactation and placentation. PLoS Biol. 2008;6(3):e63.
141. Schneider WJ. Receptor-mediated mechanisms in ovarian follicle and oocyte development. Gen Comp Endocrinol. 2009;163(1–2):18–23.
142. Evans MI, Silva R, Burch JB. Isolation of chicken vitellogenin I and III cDNAs and the developmental regulation of five estrogen-responsive genes in the embryonic liver. Genes Dev. 1988;2(1):116–24.
143. Philipsen JN, Hennis BC, Ab G. In vivo footprinting of the estrogen-inducible vitellogenin II gene from chicken. Nucleic Acids Res. 1988;16(20):9663–76.
144. Mazanko MS, Makarenko MS, Chistyakov VA, Usatov AV, Prazdnova EV, Bren AB, et al. Probiotic intake increases the expression of vitellogenin genes in laying hens. Probiotics Antimicrob Proteins. 2019;11(4):1324–9.

## Publisher's Note